ANL-HEP-PR-95-84
-HEP-95-28

Institute for Fundamental Theory Preprint UFIFT

Polarized and Unpolarized Double Prompt Photon Production in Next-to-Leading Order QCD

Claudio Corianò[a], and L. E. Gordon[b]

[a] *Institute for Fundamental Theory, Physics Department, University of Florida at Gainesville, 32611, FL, USA*

[b] *High Energy Physics Division, Argonne National Laboratory, Argonne, IL 60439, USA*

Abstract

We calculate $O(\alpha_s)$ corrections to inclusive and isolated double prompt photon production, both for the unpolarized case, and for longitudinal polarization of the incoming hadrons. The calculation is performed using purely analytical techniques for the inclusive case, and a combination of analytical and Monte Carlo techniques to perform the phase space integration in the isolated case. A brief phenomenological study is made of the process $pp \to \gamma\gamma X$ at CMS energies appropriate for the RHIC heavy ion collider.

Typeset using REVTEX

I. INTRODUCTION

Among the various and still unexplained aspects of QCD, the study of the spin structure of the nucleon has gathered considerable work in recent years [1], suggesting that a simple parton model interpretation of the phenomenon is far too simplified to completely describe the distribution of spin inside the nucleons. The original EMC data suggested that quark spin accounts for only a small fraction of the nucleon spin. Since then the possibility that gluons may carry a significant fraction of the nucleon's spin has been advanced and investigated theoretically (see [2] and Refs. therein). But other alternative explanations, such as the possibility that the proton may have a large negative strange sea polarization have also been suggested, along with various scenarios which use a combination of the two extremes.

Recently, new experimental results on the polarized proton structure function g_1^p have become avaliable [3]. Most of the information collected so far from the phenomenological side, which however still leaves an appreciable disagreement with naive parton model expectations, is based on studies of the hadronic tensor in the kinematic region of Deep Inelastic Scattering (DIS), through its structure functions $g_1^p(x, Q^2)$ (x is the Bjorken variable), primarily at large Q^2 and finite x. This discrepancy, referred to by some as "the spin crisis", indicates that sum rule predictions [4], based on the constituent quark model picture of the nucleon, need to be amended, since it is only in the DIS limit that the structure functions - which parametrize the hadronic tensor - scale to quark distributions which are functions of x only.

At finite Q^2, DIS sum rules are violated by quark-gluon interactions, usually parameterized by higher twist effects in the Operator Product Expansion. The contribution coming from the axial anomaly [2] (see also [5] and Refs. therein), in particular, has been shown to induce a cancellation between quark and gluon contributions to the first moment of the polarized structure function, $g_1^p(x)$.

Although the anomalous contribution is a radiative effect ($O(\alpha_s)$), renormalization group arguments and the $\log(Q^2)$ increase of the nucleon spin suggest that such contribution (which

is $\alpha_s(Q^2)\Delta G$) remains finite even in the $Q^2 \to \infty$ limit in which the O.P.E. is applicable. The "spin crisis" is therefore solved by the observation that the EMC result is *not* a measure of the quark spin, according to the naive parton model picture. It only measures the combination

$$\frac{1}{9}\left(\Delta\Sigma - \frac{3\alpha_s}{2\pi}\Delta G\right)$$

between the quark $\Delta\Sigma$ and the gluon contributions to the total spin. This leaves open the question as to the actual size of ΔG, i.e. whether it is large or small. This question can only be settled conclusively by experiments which are capable of directly probing ΔG.

Given the universality of the structure functions within QCD, it is expected, in a few years from now, that the information gained from DIS polarized scattering will be supported and supplemented by new results from polarized proton-proton collisions at the BNL heavy ion collider RHIC in forthcoming experiments. It is therefore important and interesting to see how various processes at large p_T are affected -in the polarized case- in their behaviour when next-to-leading (NLO) order corrections are included. It is also interesting to see how the asymmetry between the unpolarized and the polarized cross sections behaves when a reduced scale dependence is present, due to firmer NLO perturbative calculations. From the theoretical side, further motivation to proceed with these studies comes from the fact that the splitting functions for a complete NLO Q^2-evolution of the spin structure function g_1 have been recently obtained [6], and new parametrizations in NLO will soon be available for the first time. Many processes have been suggested for study at RHIC [7], but only a few so far have been calculated at NLO [8, 9].

In this work we present a next-to-leading order study of the process $pp \to \gamma\gamma X$, which has been calculated in the past [10] for unpolarized photons at NLO. We repeat both these calculations and extend them to the polarized case, which to our knowledge has only been studied in LO [11], with inclusion of the higher order ($O(\alpha_s^2)$) process $gg \to \gamma\gamma$. There it was found that the cross section should be large enough to measure, and should have some sensitivity to the polarized parton distributions but that the asymmetries are not very large except in regions where sea quark spin dependent processes dominate. This meant that

the process would not be useful for extracting information on ΔG. But they also made the point that a full NLO study including all relevant contributions would be necessary to confirm these conclusions, since cancellations between the various processes may occur, and the effect of the corrections were completely unknown. For example, they could not include contributions for the higher order process $qg \to \gamma\gamma q$, which are known to be quite significant, and can even be larger than the $q\bar{q}$ scattering process in proton-proton collision processes, as opposed to proton-anti-proton collision processes. Also, in addition to the possibility that double prompt photon production may yield important information on the polarized proton structure function, particularly the possibility that a large fraction of proton spin is carried by gluons, or a large negatively polarized strange sea, the process is also important because it is a background to Higgs decay. A full NLO analysis using more modern polarized parton distribution is now necessary to either support or disagree with the conclusions of Ref.[11]. In this study we are not yet able to use parton distributions evolved in NLO as these are not yet ready, but in a future study we hope to include them [12]. We can nevertheless extend that of Ref.[11], by including all $O(\alpha_s)$ higher order corrections to the hard scattering process and correctly taking isolation effects into account.

The organization of the paper is as follows. In section II we describe the methods involved in the calculation and the regularization prescriptions adopted for the inclusive case. The main contribution of this paper is the calculation of the polarized cross section, but since the unpolarized cross section has been presented before, we discuss this first in each case and then extend the arguments to the polarized case. In section III we outline the combined analytic/Monte Carlo method of calculating the isolated cross section. In section IV we present and discuss some numerical results, and in section V we draw some conclusions.

II. INCLUSIVE DOUBLE PHOTON PRODUCTION

The inclusive cross section we calculate is

$$\frac{d\sigma}{dk_{T1}^{\gamma} dy_1^{\gamma} dz}$$

This cross section is differential in the transverse momentum, k_{T1}^{γ}, and rapidity of one of the photons (referred to as the trigger photon) plus the variable z defined by

$$z = -\frac{k_{T1}^{\gamma}.k_{T2}^{\gamma}}{|k_{T1}^{\gamma}|^2}. \tag{2.1}$$

z thus contains information about the transverse momentum of the second photon, but not its rapidity. The cross section is thus limited in that experimental cuts on the rapidity of the second photon and isolation cuts on either photon cannot be implemented. It is nevertheless still worth calculating, since it provides a check on the more versatile calculation using combined analytic and Monte Carlo techniques which we describe in section III.

A. LO Contributions

In LO $O(\alpha_{em}^2)$, the contributions to double prompt photon production are from $q\bar{q}$ annihilation to two photons, and the various single and double fragmentation contributions, some of which are shown in Fig.1. From Eq.(2.1) we can see that the $q\bar{q}$ annihilation process in LO is proportional to $\delta(1-z)$, as the $k_T's$ of the two photons must balance. The hard subprocess cross section is

$$\frac{d\hat{\sigma}}{dvdwdz}(q\bar{q} \to \gamma\gamma) = \frac{2\pi\alpha_{em}^2}{3\hat{s}} e_q^4 \frac{1-2v+2v^2}{v(1-v)} \delta(1-z)\delta(1-w) \tag{2.2}$$

where

$$\begin{aligned} v &= 1 + \frac{t}{s} \\ w &= \frac{-u}{s+t}, \end{aligned} \tag{2.3}$$

α_{em} is the electromagnetic coupling constant and e_q denotes the quark charge. The usual Mandelstam invariants are defined in terms of the momenta of the two incoming hadrons P_A and P_B, the momentum fractions of the initial partons x_1 and x_2, and the momentum of the trigger photon k_1 via,

$$s = (x_1 P_A + x_2 P_B)^2 = x_1 x_2 S$$

$$t = (x_1 P_A - k_1)^2$$
$$u = (x_2 P_B - k_1)^2 \tag{2.4}$$

where $\sqrt{S}$ is the center-of-mass energy in the hadronic system.

In this study we do not include contributions where both photons are produced by fragmentation off a final state parton as these are expected to give a very small contribution, especially after isolation effects are considered. We do include process where one of the photons is produced directly and the other by fragmentation, referred to as the single fragmentation contributions (Fig.1b). These processes contribute to $O(\alpha_{em}^2)$, although the hard subprocess is $O(\alpha_s \alpha_{em})$, since the fragmentation function of parton i into a photon, $D_{\gamma/i}(z, Q^2)$ is $O(\alpha_s/\alpha_{em})$. In a fully consistent NLO calculation we should also include the $O(\alpha_s)$ corrections to these fragmentation processes, but we are not yet in a position to provide these.

The full expression for the physical $q\bar{q}$ annihilation cross section in LO is

$$\frac{d\sigma}{dk_{T1}dy_1dz} = \frac{2\pi k_{T1}}{\pi S}\int_{VW}^{V}\frac{dv}{1-v} f_q^A(x_1, M^2) f_{\bar{q}}^B(x_2, M^2)\frac{d\hat{\sigma}}{dvdwdz}(q\bar{q} \to \gamma\gamma) + (q \leftrightarrow \bar{q}), \tag{2.5}$$

where V and W are defined similarly to v and w in Eq.(2.3) except now in the hadronic system, and $f_i^A(x, M^2)$ is the parton distribution function for parton of type i in hadron A as a function of x, the momentum fraction, and the scale, M^2.

There are two types of single fragmentation contributions to the process. Those where the trigger photon γ_1 is produced by fragmentation and those where γ_2 is. These contribute in different regions of z, the former in the region $z \geq 1$ and the latter in the region $z \leq 1$. In terms of the hard subprocess cross sections for the processes $q\bar{q} \to \gamma g$ and $qg \to \gamma q$ which can be found, for example in Ref.[10], these contributions are given by the expressions;

$$\frac{d\sigma}{dk_{T1}dy_1dz} = 2\pi k_{T1}\frac{1}{\pi S}\sum_{i,j,l}\int_{1-V+VW}^{1}\frac{dz'}{z'^2}\int_{VW}^{V}\frac{dv}{1-v} f_i^A(x_1, M^2) f_j^B(x_2, M^2)\frac{d\hat{\sigma}^{ij\to\gamma_2 l}}{dv}$$
$$D_{\gamma_1/l}(z', M_F^2)\theta(z-1)\delta(\frac{1}{z} - z'), \tag{2.6}$$

and

$$\frac{d\sigma}{dk_{T1}dy_1dz} = 2\pi k_{T1}\frac{1}{\pi S}\sum_{i,j,k}\int_{1-V+VW}^{1}\frac{dz'}{z'^2}\int_{VW}^{V}\frac{dv}{1-v}f_i^A(x_1,M^2)f_j^B(x_2,M^2)\frac{d\hat{\sigma}^{ij\to\gamma_1 k}}{dv}$$
$$D_{\gamma_2/k}(z',M_F^2)\theta(1-z)\delta(z-z'), \tag{2.7}$$

where i,j and k run over the various quark flavours and the gluon and M_F^2 is the fragmentation scale.

In the polarized case the cross sections are given by the same expressions as above, but now the hard subprocess cross sections must be replaced by the corresponding polarized ones, $d\Delta\hat{\sigma}/dv$. The parton distributions must also be replaced by the corresponding polarized ones which are defined by

$$\Delta f_a^A(x,Q^2) = f_{a,+}^A(x,Q^2) - f_{a,-}^A(x,Q^2) \tag{2.8}$$

where $f_{a,\pm}^A(x,Q^2)$ is the distribution of parton of type a with positive $(+)$ or negative $(-)$ helicity in hadron A. Likewise the polarized subprocess cross sections are defined by

$$\frac{d\Delta\hat{\sigma}}{dv} = \frac{d\hat{\sigma}}{dv}(+,+) - \frac{d\hat{\sigma}}{dv}(+,-). \tag{2.9}$$

Again, $+,-$ denote the helicities of the incoming partons. Since only the initial state is polarized, we do not need to change the photon fragmentation functions. The hard subprocess cross sections in LO for these can be found, for example, in Ref.[9].

B. The Box Diagram

At collider energies, the box diagram process, $gg \to \gamma\gamma$ (Fig.1c), although it is $O(\alpha_s^2\alpha_{em}^2)$, has been shown to contribute significantly to the cross section for unpolarized double prompt photon production in the low k_T region due to the large gluon distribution at low-x. It is questionable whether or not one should include contributions from the box diagram in an $O(\alpha_s)$ NLO calculation, since it is of higher order, and may introduce numerical cancellations with the genuine NLO contributions leading to misleading results. In a proper phenomenological study at NLO we would not include this contribution, but in order to make contact with the work of Ref.[12], and to estimate the contribution from this process, we will include

it. The unpolarized hard subprocess has been used many times before and can be found, for example, in Ref.[13]. For the polarized case the hard subprocess cross section can be obtained from the amplitudes according to the prescription given in Ref.[11]. To calculate the contribution form this process, we use a similar expression to Eq.(2.5), with the quark distributions replaced by gluon distributions and the hard subprocess cross section replace by that for the $gg \to \gamma\gamma$ one.

C. The NLO contributions

At NLO $O(\alpha_{em}\alpha_s)$ there are the virtual gluon corrections to the LO $q\bar{q}$ annihilation process, plus real gluon emission corrections $q\bar{q} \to \gamma\gamma g$ (Fig.(2)). In addition, the 3-body process $qg \to \gamma\gamma q$ also contributes (Fig(3)). The virtual contributions can be obtained directly from Ref.[9], where they were calculated for single prompt photon production in both the polarized and unpolarized cases, by simply removing the non-abelian couplings. The 3-body matrix elements can be obtained in a similar way.

A note concerning the matrix elements for the polarized case is in order here. When taking the traces to calculate the helicity dependent matrix elements, one needs to project onto definite helicity states, labelled h for quarks and λ for gluons, for the incoming particles. This is achieved for quarks by defining spinors of definite helicity according to

$$u(p_1,h)\bar{u}(p_1,h) = \frac{1}{2}\gamma^\mu(p_1)_\mu(1-h\gamma_5) \tag{2.10}$$

where p is the momentum. For gluons the general expression is

$$\epsilon_\mu(p_2,\lambda)\epsilon^*_\nu(p_2,\lambda) = \frac{1}{2}\left[-g_{\mu\nu} + i\lambda\epsilon_{\mu\nu\rho\sigma}\frac{p_2^\rho p_1^\sigma}{p_1.p_2}\right]. \tag{2.11}$$

This introduces the γ_5 matrix and the antisymmetric tensor $\epsilon_{\mu\nu\rho\sigma}$ which are defined in 4-dimensions. To work in $n \neq 4$-dimensions, some consistent scheme must be chosen in which to treat these 4-dimensional objects. In Ref.[9], the original scheme of t'Hooft and Veltman [14], and Breitenlohner and Maison [15] was chosen. Briefly, this scheme makes a division of n-dimensional Minkowski space into a 4-dimensional and a $(n-4)$-dimensional part. Thus

an arbitrary vector p will have a 4-dimensional part, $\hat{\hat{p}}$, and an $(n-4)$-dimensional part, $\hat{p}$. This means that scalar products of these 'hat' momenta will inevitably be present when traces are taken. These terms in the matrix elements must be treated properly when phase space integrals are performed. We shall consider this point in detail in appendices B and C.

In order to obtain a cross section differential in k_{T1}, y_1 and z, we need to integrate 3-body phase space over the kinematic variables of the unobserved quark or gluon. The method of performing these integrals have been detailed in Ref.[10]. We outline the method again in Appendix B and extend it to the polarized case where 'hat' momenta must also be considered. As in Ref.[10], we restrict ourselves to the cases where the photons are in opposite hemispheres, i.e. $z \geq 0$. The phase space integrals are performed in $4-2\epsilon$ dimensions in order to expose soft and collinear singularities as poles in ϵ.

In the case of $q\bar{q}$ scattering, we obtain single and double poles in ϵ from the 3-body phase space integrals. When the virtual contributions are added to this the double poles automatically cancel and the remaining single poles must be absorbed into the parton distribution functions. Thus there are three pieces to our calculation for this process which must be combined in order to get a finite partonic subprocess cross section. There is the virtual contribution which we represent by the function

$$\frac{d\sigma^V_{q\bar{q}}}{dvdwdz}\left(\hat{s}, v, z, \frac{1}{\epsilon^2}, \frac{1}{\epsilon}\right).$$

There is the result of integrating the 3-body matrix element over the phase space of the unobserved partons as described in appendices B and C, which we denote by the function

$$k'_{q\bar{q}}\left(\hat{s}, v, w, z, \frac{1}{\epsilon^2}, \frac{1}{\epsilon}\right).$$

and there is the factorization counter term

$$\frac{1}{\hat{s}v}\frac{d\sigma^F_{q\bar{q}}}{dvdwdz} = -\frac{\alpha_s}{2\pi}\left[\frac{1}{1-vw}H_{qq}\left(\frac{1-v}{1-vw}, M^2\right)\frac{d\sigma^{q\bar{q}\to\gamma\gamma}}{dv}\left(\frac{1-v}{1-vw}\hat{s}, vw, \epsilon\right)\delta(1-z)\right.$$
$$\left.\frac{1}{v}H_{qq}(w, M^2)\frac{d\sigma^{q\bar{q}\to\gamma\gamma}}{dv}(w\hat{s}, v, \epsilon)\delta(1-z)\right], \qquad (2.12)$$

where

$$H_{ij}(z,Q^2) = -\frac{1}{\hat{\epsilon}} P_{ij}(z) \left(\frac{\mu^2}{Q^2}\right) + f_{ij}(z). \tag{2.13}$$

In the $\overline{MS}$ factorization scheme which we adopt, $1/\hat{\epsilon} = 1/\epsilon - \gamma_E + \ln 4\pi$, $f_{ij}(z) = 0$, and $P_{ij}(z)$ are the well known one-loop splitting functions for parton j into parton i [16]. The finite subprocess cross section is now obtained by adding these three parts,

$$\begin{aligned} K_{q\bar{q}}(\hat{s},v,w,z,M^2) = k'_{q\bar{q}}\left(\hat{s},v,w,z,\frac{1}{\epsilon^2},\frac{1}{\epsilon}\right) + \frac{d\sigma^V_{q\bar{q}}}{dvdwdz}\left(\hat{s},v,z,\frac{1}{\epsilon^2},\frac{1}{\epsilon}\right) \\ + \frac{1}{\hat{s}v}\frac{d\sigma^F_{q\bar{q}}}{dvdwdz}\left(\hat{s},v,w,z,\frac{1}{\epsilon},M^2\right), \end{aligned} \tag{2.14}$$

where M^2 is the factorization scale.

A similar procedure is followed for the qg initiated process, except now there are now no virtual contributions and hence no double poles. Also different singularities are encountered when integrating the 3-body matrix elements, hence we have a different factorization formula;

$$\begin{aligned} \frac{1}{\hat{s}v}\frac{d\sigma^F_{qg}}{dvdwdz} = -\frac{\alpha_s}{2\pi}\Bigg[& \frac{1}{1-v+vw}\tilde{H}_{\gamma q}\left(1-v+vw,M_F^2\right)\frac{d\sigma^{gq\to\gamma q}}{dv}\left(\hat{s},\frac{1-v}{1-v+vw},\epsilon\right)\delta(z_1-z) \\ & \frac{1}{v}H_{qg}(w,M^2)\frac{d\sigma^{q\bar{q}\to\gamma\gamma}}{dv}(w\hat{s},v,\epsilon)\delta(1-z) \\ & + \frac{1}{v}\tilde{H}_{\gamma q}\left(z,M_F^2\right)\frac{d\sigma^{gq\to\gamma q}}{dv}(\hat{s},v,\epsilon)\,\delta(1-w)\theta(1-z)\Bigg]. \end{aligned} \tag{2.15}$$

where

$$\tilde{H}_{\gamma q}(x,M_F^2) = -\frac{1}{\hat{\epsilon}} P_{\gamma q}(z)\left(\frac{\mu^2}{M_F^2}\right), \tag{2.16}$$

M_F is the fragmentation scale and $z_1 = 1/(1-v+vw)$.

Once $(\Delta)K_{q\bar{q}}$ and $(\Delta)K_{qg}$ have been calculated then we can use them to calculate the physical cross sections by convoluting them with the appropriate parton distribution functions. In both the polarized and unpolarized cases the general formula is

$$\begin{aligned} \frac{d(\Delta)\sigma}{dk_{T1}dy_1dz} = 2\pi k_{T1}\frac{1}{\pi S}\sum_{i,j}\int_{VW}^1\frac{dv}{1-v}\int_{VW/v}^1\frac{dw}{w}f_i^A(x_1,M^2)f_j^B(x_2,M^2) \\ \left[\frac{1}{v}\frac{d(\Delta)\hat{\sigma}^{ij}}{dv}\delta(1-z)\delta(1-w) + \frac{\alpha_s(\mu^2)}{2\pi}(\Delta)K_{ij}(\hat{s},v,w,z,M^2,M_F^2)\right]. \end{aligned} \tag{2.17}$$

The indices i, j run over quark flavours or represent a gluon, and in the case of $q\bar{q}$ scattering, the first term is the LO contribution, which is absent for the qg initiated process.

III. MONTE CARLO CALCULATION

The combination of analytic and Monte Carlo techniques used here to perform the phase space integrals has been documented and described in detail elsewhere (see Bailey *et al.*,[10] and references therein), so our discussion will be fairly brief, highlighting mostly those features which are important to our calculation. The basic technique comprises isolating those regions of phase space where soft and collinear singularities occur and integrating over them analytically in $4 - 2\epsilon$ dimensions. In this way the singularities are exposed as poles in ϵ. These regions are isolated form the rest of the 3-body phase space by the imposition of arbitrary boundaries between them, achieved by introducing cut-off parameters. The soft gluon region of phase space is defined to be the region where the gluon energy, in a specified reference frame, usually the subprocess rest frame, falls below a certain threshold, $\delta_s\sqrt{\hat{s}}/2$, where δ_s is the arbitrary cut-off parameter and $\hat{s}$ is the center-of-mass energy in the parton-parton system. If we label the momenta for the general 3-body process by $p_1 + p_2 \to p_3 + p_4 + p_5$, then we can define the general invariants by $s_{ij} = (p_i + p_j)^2$ and $t_{ij} = (p_i - p_j)^2$. The collinear region is then defined as the region where the value of an invariant falls below the value $\delta_c\hat{s}$.

The phase space integration over the mutually exclusive soft and collinear regions are performed not on the full matrix elements but on approximate versions of them defined in specific ways. In the soft gluon case they are obtained by setting the gluon energy to zero everywhere where it occurs in the matrix elements, except in the denominators. This is the soft gluon approximation. Similarly, in the collinear case, each invariant which vanishes is in turn set to zero everywhere except in the denominator. This is the leading pole approximation. The phase space integrals are then performed on these and only the logarithms of the cut-off parameters are retained. All positive powers of the cut-off parameters are set to

zero. The meaning of all this is that for the method to work the parameters must be kept small, otherwise the approximations made will no longer be valid and the method would fail.

Once the phase space integrals have been performed and the soft and collinear poles are exposed, then the virtual contributions, if any, are added to them, at which time all double poles and single poles of soft (IR) origin automatically cancel. The remaining collinear poles are then factorized in the parton distribution and fragmentation functions in the usual way, at some scale and using some specific factorization scheme. In our case we use the $\overline{MS}$ scheme. At this point one is left with a set of 2-body processes which depend explicitly on $\ln \delta_s$ and $\ln \delta_c$, and a set of 3-body matrix elements which when integrated over the phase space using Monte Carlo techniques, have an implicit dependence on these same logarithms, but which now have opposite signs in order to cancel the dependence in the 2-body part. The physical cross sections will then be independent of these arbitrary cut-off parameters.

It is generally very simple to impose experimental cuts and to calculate different observables when one is dealing with 2-body matrix elements only, as in the usual LO calculations. This is not the case when we consider 3-body processes, as there is the need now to cancel soft and collinear divergences, but beyond that, the standard techniques require often complex Jacobian transformations to calculate cross sections differential in different variables, and the phase space integrals can sometimes only be done analytically when specific limits of integration are involved. This can sometimes make in impossible to impose cuts on the kinematic variables. Thus, fully analytic methods of performing calculations for physical processes, although in some cases desirable, can be rather restricted in their usefulness when confronted with experimental situations where it is often desirable and sometimes even unavoidable that cuts be made. The combined analytic and Monte Carlo method does not suffer from these particular drawbacks, in that it is very easy to calculate cross sections differential in many different variables at once, and cuts on the kinematic variables to match those made in the experiments can be easily imposed because the phase space integrals are performed numerically after all singularities have been dealt with.

Our calculation of double prompt photon production proceeds along exactly the same lines to that described in the second of Ref.[10]. In fact the only difference is that in the polarized case we must deal with 'hat' momentum integrals as outlined in section II. It turns out that the 'hat' momenta only contribute in the collinear limit when an initial state parton splits into two partons, one of which participates in the hard scattering. This point is discussed in fair detail in Ref.[9], where it was suggested that, since these contributions seem to be of the same form for a particular vertex in the collinear limit, they may be regarded as universal properties of these parton legs in the HVBM scheme, and as such may be factorized into the parton distributions under a new ($\overline{MS}_p$) factorization scheme. In our calculation, we choose not to use this scheme because the new polarized parton distributions are being calculated in the standard $\overline{MS}$ scheme. Thus, these contributions are included in our 2-body part on the cross section.

Thus all the discussion in Ref.[10] on the Monte Carlo method can be carried directly over to the polarized case, expect that once factorization has been performed the expression for the remnants of the hard collinear singularities is now given for the polarized case by

$$\begin{aligned}\frac{d\Delta\tilde{\sigma}}{dv}(q\bar{q}\to\gamma\gamma) = \frac{\alpha_s}{2\pi}\frac{d\Delta\sigma^{Born}}{dv} \\ \times\Bigg[&\Delta f_q^A(x_1,M^2)\int_{x_2}^{1-\delta_s}\frac{dz}{z}f_{\bar{q}}^B(x_2/z,M^2)\Delta\tilde{P}_{qq}(z) \\ &+\Delta f_q^A(x_1,M^2)\int_{x_2}^{1}\frac{dz}{z}f_g^B(x_2/z,M^2)\Delta\tilde{P}_{qg}(z) \\ &+\Delta f_{\bar{q}}^B(x_2,M^2)\int_{x_1}^{1-\delta_s}\frac{dz}{z}f_q^A(x_1/z,M^2)\Delta\tilde{P}_{qq}(z) \\ &+\Delta f_{\bar{q}}^B(x_2,M^2)\int_{x_1}^{1}\frac{dz}{z}f_g^A(x_1/z,M^2)\Delta\tilde{P}_{qg}(z)\Bigg] \end{aligned} \tag{3.1}$$

with

$$\Delta\tilde{P}_{ij}(z) = \Delta P_{ij}(z)\ln\left(\frac{1-z}{z}\delta_c\frac{\hat{s}}{M^2}\right) - \Delta P'_{ij}. \tag{3.2}$$

The polarized Altarelli-Parisi splitting functions in $4-2\epsilon$ dimensions are

$$\Delta P_{qq}(z,\epsilon) = C_F\left[\frac{1+z^2}{1-z} + 3\epsilon(1-z)\right], \tag{3.3}$$

and

$$\Delta P_{qg}(z,\epsilon) = \frac{1}{2}\left[(2z-1) - 2\epsilon(1-z)\right]. \tag{3.4}$$

Part of the second terms in the splitting functions come from the 'hat'-momenta as discussed in Ref.[9]. The functions $\Delta P'_{ij}$ are defined by the relation,

$$\Delta P_{ij}(z,\epsilon) = \Delta P_{ij}(z) + \epsilon \Delta P'_{ij}(z). \tag{3.5}$$

IV. NUMERICAL RESULTS

In this section we present some numerical results for polarized and unpolarized double prompt photon production at RHIC center-of-mass energies. We first study the non-isolated cross section, since we do not know what isolation restrictions will be necessary at RHIC. We will then present some results for the isolated cross section, assuming some plausible isolation parameters, based on those used by the CDF collaboration at Fermilab.

Throughout we use the GRV [17] parton distributions for the proton in the unpolarized case. We use $\Lambda^{(4)}_{QCD} = 0.200$, to match the GRV parton distributions, but we do not include any contribution for charm quarks, since these are not included in the polarized parton distributions. For the polarized parton distributions we use the two sets proposed by Cheng and Wai [18]. In the first set which we will refer to as scenario *a*, a large polarized gluon distribution is assumed, and the SU(3) flavour symmetric sea quark distribution is assumed to vanish at the input scale. In the other case (scenario *b*), the gluon distribution vanishes at the input scale, but the SU(3) flavour symmetric polarized sea quark distribution is assumed to be directly related to the unpolarized strange sea, leading to a large negatively polarized sea, and small polarized gluon distributions. In both cases the valence distributions are assumed proportional to the unpolarized ones. The main aim of this paper is not to provide the most up to date phenomenological study of the polarized cross section, but to gauge the importance of higher order corrections and make contact with the results of Ref.[12]. We are also interested in whether the cross section is sensitive to ΔG, hence the use of the Cheng and Wai distributions which have extreme gluon distributions.

For the electromagnetic coupling constant we use $\alpha_{em} = 1/137$ and we use the two loop expression for $\alpha_s(\mu^2)$. Unless otherwise stated, we set all factorization/renormalization scales to $\mu^2 = ((k_{T1}^\gamma)^2 + (k_{T2}^\gamma)^2)/2$. We make use of the asymptotic parametrizations for the parton to photon fragmentation functions provided in Ref.[13]. We assume the maximum $\sqrt{S} = 500\ GeV$ for the RHIC centre-of-mass energy.

In a future study [12] we will use photon fragmentation functions evolved in NLO, polarized parton distributions evolved in NLO as well as including a contribution from charm quarks. There we hope to make up-to-date estimates of the cross section ate RHIC.

A. The Inclusive Cross Section

In the analytic calculation of the inclusive cross section, we exposed the various soft and collinear poles by expanding the integrated matrix elements as plus-distributions in the variable z. The details are given in the Appendix. This procedure ensures that these integrable singularities can be treated numerically, but it prevents us from providing distributions in the z-variable with infinitely sharp resolution. That is, in order for us to present finite z-distributions in we must integrate over some finite range of z. Following the procedure used in Ref.[10], we define

$$\frac{d(\Delta)\sigma}{dk_{T1}^\gamma dy_1 dz} = \frac{1}{\Delta z}\int_{z-\frac{\Delta z}{2}}^{z+\frac{\Delta z}{2}} \frac{d(\Delta)\sigma}{dk_{T1}^\gamma dy_1 dz'} dz', \tag{4.1}$$

and provide the distributions in z with finite bin widths Δz. For the k_T distributions we integrate over a specified range of z,

$$\frac{d(\Delta)\sigma}{dk_{T1}^\gamma dy_1} = \int_{z_a}^{z_b} \frac{d(\Delta)\sigma}{dk_{T1}^\gamma dy_1 dz} dz. \tag{4.2}$$

In fig.4a we show the z-distribution for the unpolarized cross section, at $k_{T1}^\gamma = 5\ GeV$ and $y_1 = 0$, for a bin size $\Delta z = 0.2$. The LO Born term gives a sharp peak at $z = 1$ but the effect of the higher order corrections is to reduce and broaden this peak. The higher order correction terms, neglecting the gg process which is positive and contributes only at $z = 1$, give a negative contribution at $z = 1$, as indicated by the dashed line. It turns out that

the fragmentation terms where the trigger photon is produced via fragmentation give large contributions in the region $z \leq 1$, whereas those where the other photon is produced in this way give a positive but not as large contribution at $z \geq 1$. This is partly due to the fact that phase space runs out in this region. The overall shape of the distribution is similar to that obtained in Ref.[10].

In Fig.4b we compare the polarized and unpolarized cross sections with the same parameters as in fig.4a. The unpolarized cross section is scaled by a factor of 1/10 for easier comparison. In general the curves have a similar shape, but due to cancellation between various parts of the polarized cross section, it has a much more sharply pronounced peak at $z = 1$.

The k_T distribution is displayed in fig.5a for $0.2 \leq z \leq 2.0$ and $|y_1| \leq 3$. The solid curve is the unpolarized cross section, while the dashed and dotted curves are the polarized cross sections for scenario a and b respectively. Clearly, given a reasonably large luminosity, the cross sections are large enough to measure out to a k_T of about 50 GeV say. Also the two scenarios give significantly different predictions indicating sensitivity to the polarized distributions. The main question is the sensitivity of the cross section to polarization. To determine this we plot the longitudinal asymmetry A_{LL} defined by

$$A_{LL} = \frac{\frac{d\Delta\sigma}{dk_{T_1}^{\gamma} dy_1^{\gamma}}}{\frac{d\sigma}{dk_{T_1}^{\gamma} dy_1^{\gamma}}}. \tag{4.3}$$

The dotted curve shows the asymmetry predicted for the Born cross section using the parton distributions of scenario a. At the hard parton-parton scattering level this asymmetry is $A_{LL} = -1$, and is thus modified significantly by folding with the parton distributions. Note that this is not the asymmetry for the LO cross section, since we have not included the contributions from photon fragmentation. The solid and dashed curves give the asymmetry of the full higher cross section for scenario a and b respectively. In the case of scenario a, the asymmetry is already about 10% at $k_T = 15$ GeV, and rises to nearly 20% at $k_T = 50$ GeV. For scenario b the asymmetry is more modest, varying between 4 and 9% for a similar range in k_T. Thus, the inclusive cross section is sensitive to the polarized parton distributions

used, and the asymmetry not too small in some accessible kinematic regions.

Of course as we have stated before the inclusive cross section we have calculated is probably not going to be of much practical use at the RHIC collider due to the need to isolate in order to identify the photon signal. Its main usefulness is as a check on the more versatile calculation using Monte Carlo techniques which we shall discuss in the next section.

B. The Isolated Cross Section

In this section we study the isolated cross section for double prompt photon production at RHIC. We keep all distributions and parameters the same as for the inclusive case, but in addition a cone size of $R = 0.7$ and an energy resolution parameter $\epsilon = 2\ GeV/k_T^\gamma$ is used. The cone of radius R, with the photon at the centre, is defined in the pseudorapidity-azimuthal angle plane ($y - \phi$-plane) by the relation

$$R = \sqrt{(\Delta y)^2 + (\Delta\phi)^2}.$$

If hadronic energy greater than a fraction ϵ of the photon energy is observed in the cone then the event is rejected. This serves to define the isolated cross section.

In fig. 6a we display the k_T distribution of the full isolated polarized and unpolarized cross sections. Note that this curve cannot be directly compared with that in fig.5a since here the cuts are different. In fig.6a both photons are still allowed to have rapidities in the range $|y^\gamma| \leq 3$, but for a fixed k_T of one of the photons which we plot vs cross section, the other is allowed to have $k_T \geq 5\ GeV$. Our predictions indicate a measurable cross section out to k_T around 30 to 40 GeV, given enough luminosity. Again, in the polarized case, sensitivity to the polarized parton distribution chosen is evident from the figure.

Fig.6b shows the asymmetries of the cross sections in fig.6a for scenarios *a* and *b*. There is a very pronounced difference in the asymmetries for scenarios *a* vs *b*, indicating a corresponding sensitivity to the polarized parton distributions. The implication of these results is that discrimination between the two extreme cases presented here should be possible from

measurement of this cross section with moderately good statistics at RHIC. In fig.6c we break down the asymmetry in the various initial state contributing processes for the case of scenario a. The gg initiated process, as expected, only gives a significant contribution at low k_T due to the steeply falling gluon distribution. But we find that for this scenario the asymmetry is dominated by the qg initiated process. We did a similar analysis for scenario b and found that the contribution from the $q\bar{q}$ initiated process was largest and that from the gg initiated process was completely negligible. The cross section is thus very sensitive to the size of ΔG.

In fig.7 we show the scale dependence of the isolated cross section, with the same cuts as above, for the unpolarized case. We chose three different scales $\mu^2 = n^2((k_{T1}^{\gamma})^2 + (k_{T2}^{\gamma})^2)/2$, where $n = 1, 1/2$ and 2. All factorization/renormalization scales are varied simultaneously. There is obviously some dependence of the cross section on the scales chosen, leading to an estimated 20% uncertainty in our predictions at $k_T = 15\ GeV$.

Lastly in fig.8 we show the k_T distribution of the cross section for unpolarized isolated double prompt photon production for the same cuts chosen above but at a cms energy of $\sqrt{S} = 14\ TeV$ appropriate for the LHC collider. The cross section is as expected much larger than at lower energies and even at $k_T = 100\ GeV$ we can expect a cross section of more than 0.1 pb.

V. CONCLUSIONS

In this paper we calculated the cross section for polarized and unpolarized double prompt photon production in pp collisions at cms energies appropriate for the RHIC collider. We examined whether the isolated cross section is sensitive to the spin dependent gluon distributions of the proton, by comparing two extreme (LO) parametrizations of ΔG. Our results indicate that the cross section is large enough to measure, and that it should indeed be sensitive to the polarized gluon distributions leading to the possibility that it may be useful to help discriminate between some extreme scenarios for the polarized distributions. Our

results differ from those reached in a previous ,mostly LO, study in that we find a significant contribution to the asymmetry from the qg initiated process, leading to a corresponding sensitivity of the cross section to the polarized gluon distribution, ΔG. This cross section should therefore be useful as a supplement for information on the polarized distributions gathered from more sensitive sources such as jet or prompt photon production. The main drawback of our study is the use of rather outdated polarized parton distributions evolved in LO only. We therefore do not claim to have provided NLO estimates for the polarized cross section at RHIC, but only an indication as to the size of the cross section and sensitivity to ΔG.

Indications are that the cross section for double prompt photon production will, as expected, be sizable at the LHC, and will thus provide a significant background to Higgs searches.

VI. ACKNOWLEDGEMENTS

C.C. thanks the Theory Group at Argonne and in particular Alan White for their kind hospitality during the final stage of this work. We thank E. L. Berger, G. Bodwin, R. Field, A. White, W. Vogelsang and G. Ramsey for comments and discussions on the matter presented, and W. Vogelsang for reading the manuscript. We thank P. Ramond for illuminating discussions concerning the role of the anomalies. Finally we express our warm gratitude to Derek and Liz Kruk, Deb Petrie and Betsy Herman for encouragement. This work supported in part by the U.S. Department of Energy, Division of High Energy Physics, Contract W-31-109-ENG-38 and DEFG05-86-ER-40272.

APPENDIX A: REGULARIZATION SCHEMES

We use the γ_5 scheme of Breitenlohner and Maison [15], which is free of internal inconsistencies in the definition of γ_5 in $D-$dimensions. An anticommuting γ_5 is not compatible with Dimensional Regularization [14, 15, 21]. In the t'Hooft-Veltman scheme, systematized by Breitenlohner and Maison, an n-dimensional γ_μ matrix is split into its 4-dimensional component $\hat{\hat{\gamma}}_\mu$ and a remaining component $\hat{\gamma}$. Thus $\gamma_\mu = \hat{\hat{\gamma}}_\mu + \hat{\gamma}_\mu$. A suitable representation of γ_5 is

$$\gamma_5 = \frac{i}{4}\epsilon_{\alpha\beta\gamma\delta}\gamma^\alpha\gamma^\beta\gamma^\gamma\gamma^\delta. \tag{A1}$$

If it is postulated that γ_5 anticommute with the other 4-dimensional Dirac matrices and anticommute with the remaining ones, then all the corresponding algebraic relations can be shown to be consistent with dimensional regularization [15]. Therefore we *define*

$$\begin{aligned}\gamma_5\hat{\hat{\gamma}}_\mu + \hat{\hat{\gamma}}_\mu\gamma_5 &= 0\\ \gamma_5\hat{\gamma}_\mu - \hat{\gamma}_\mu\gamma_5 &= 0.\end{aligned} \tag{A2}$$

A discussion of the modifications which appear in the integration over the phase space of the 3 final states, due to this ansatz, is presented in the next section.

APPENDIX B: 3-PARTICLE PHASE SPACE FOR POLARIZED SCATTERINGS

As we have discussed before, the use of the t'Hooft-Veltman regularization [14] introduces a dependence of the matrix elements on the hat-momenta which requires, in part, a modification of the phase space integral which appear in the unpolarized case.

In the case of unpolarized scattering, the singularities are generated by poles in the matrix elements which have the form $1/t_3$, $1/u_3$, $1/(t_3u_3)$ and similar ones, in multiple combinations of them. Multiple poles can be reduced to sums of combinations of double poles by using simple identities among all the invariants and by the repeated use of partial

fractioning. This is by now a well established procedure. In our case we encounter new terms of the form $1/t_3^2$ and $1/u_3^2$ and new matrix elements containing typical factors of the form $\hat{\hat{k}}_3$, $\hat{\hat{k}}_2$, and $k_2 \cdot \widehat{\widehat{k}}_3$ at the numerator. Let's discuss for a moment these last terms containing hat-momenta. It is obvious that by a suitable choice of the parametrizations given by the sets 1, 2 ,3 and 4, (defined in the next section) we are able to reduce to the ordinary phase space result given by (B42) all the matrix elements containing scalar products of the form $p_i \cdot \widehat{\widehat{k}}_j$, $k_1 \cdot \widehat{\widehat{k}}_j$ with $i = 1, 2$, $j = 1, 2, 3$. Therefore it is possible to set to zero, after taking the traces, all the products contain such combinations of hat-momenta. Then, the only matrix elements of hat-momenta which are left and which are not set to zero are those containing products of the form $k_a \cdot \widehat{\widehat{k}}_b$,with $a, b = 1, 2$.

Let's consider the 3-particle phase space integral when hat-momenta are present

$$PS_3 \equiv \int d^n k_1 d^n k_3 d^n k_2 \delta(k_3^2)\delta(k_2^2)\delta(k_1^2)\delta^n(p_1 + p_2 - k_3 - k_2 - k_1)\widehat{\widehat{k}}_2^2 \qquad \text{(B1)}$$

and let's lump together the momenta k_3 and k_2 as follows

$$PS_3 = \int d^n k_1 d^n k_3 d^n k_2 d^n k_{23} \delta(k_3^2)\delta(k_2^2)\delta(k_1^2)\delta^n(p_1 + p_2 - k_2 - k_1)$$
$$\delta(p_1 + p_2 - k_1 - k_{23})\delta^n(k_3 + k_2 - k_{23})\widehat{\widehat{k}}_2^2 . \qquad \text{(B2)}$$

Eq. (B2), once integrated over k_{23}, gives (B1). We single out the invariant mass of the pair $(1, 2)$ by the relation

$$1 = \int dm^2 \delta(m^2 - k_{23}^2) \qquad \text{(B3)}$$

which we insert in (B2) to get

$$\int d^n k_1 d^n k_3 d^n k_2 d^n k_{23} dm^2 \delta(k_3^2)\delta(k_2^2)\delta(k_1^2)\delta^n(p_1 + p_2 - k_1 - k_{23})$$
$$\delta^n(k_3 + k_2 - k_{23})\delta(m^2 - k_{23}^2)\widehat{\widehat{k}}_2^2 . \qquad \text{(B4)}$$

Notice that by this trick we can factorize a 2-particle phase space

$$PS_3 = \int d^n k_1 dm^2 d^n k_{23} \delta(k_1^2)\delta(k_{23}^2 - m^2)\delta^n(p_1 + p_2 - k_1 - k_{23}) \times PS_2 \qquad \text{(B5)}$$

$$PS_2 \equiv \int d^n k_2 \delta(k_2^2)\delta((k_{23}-k_2)^2)\hat{\hat{k}}_2^2. \tag{B6}$$

We have set $k_2 = (\hat{\hat{k}}_2, \hat{k}_2)$, with

$$\hat{\hat{k}}_2 = k_2^0(1, \cos\theta_3 \sin\theta_2 \sin\theta_1, \cos\theta_2 \sin\,\theta_1, \cos\,\theta_1) \tag{B7}$$

being the 4-dimensional part of k_2. We easily get

$$\hat{\hat{k}}_2^2 = \frac{s_{34}}{4} \sin^2\theta_3\, \sin^2\theta_1\, \sin^2\theta_2. \tag{B8}$$

Therefore the usual angular integration measure

$$d\Omega^{(n-2)} = \prod_{l=1}^{n-l-2} = \sin^{n-l-2}\theta_l\, d\theta_l \tag{B9}$$

is effectively modified to

$$d\Omega^{(n-2)} = \prod_{l=1}^{3} \sin^{n-l}\theta_1 d\theta_l \times \prod_{l=4}^{n-2} \sin^{n-l-2}\theta_l d\theta_l \tag{B10}$$

This integral is evaluated in a special frame. Assuming that $k_{23}^2 > 0$, we sit in the center of mass frame of the $(1,2)$ pair, in which $k_{23} = (m, \mathbf{0})$ and $k_2 = (E_2, \mathbf{k_2})$ to get

$$\begin{aligned} PS_2 &= \int d^n k_2 \delta(k_2^2)\delta(m^2 - 2mE_2) \\ &= k_{23}^{n/2-1} I[\theta_i] \end{aligned} \tag{B11}$$

where

$$I[\theta_i] = \frac{\pi^{n/2-2}}{2^n \Gamma[n/2-2]} \int_0^\pi \sin^{n-1}\theta_1\, d\theta_1 \int_0^\pi d\theta_2 \sin^{n-2}\theta_2 \int_0^\pi d\theta_3 \sin^{n-3}\theta_3 \tag{B12}$$

where θ_1 and θ_2 are the only relevant angles which appear in the matrix elements and therefore are not integrated. We have displayed also the θ_3 integral since it is different from the unpolarized case.

After integration over m^2 and k_{23} and a simple covariantization we get

$$PS_3 = \int d^n k_1 \delta(k_1^2)[(p_1 + p_2 - k_1)^2]^{n/2-1} I[\theta_i]. \tag{B13}$$

The collinear or infrared poles are therefore isolated in the c.m. system of the pair. The remaining part of the integral is evaluated in the c.m. system of the two incoming partons p_1, p_2. At this point let's consider the sub-integral

$$I_1 = \int d^n k_1 \delta(k_1^2)[(p_1 + p_2 - k_1)^2]^{n/2-1}$$
$$= \frac{\pi^{n/2-1}}{\Gamma[n/2-1]} \int E_3^{n-3} dE_3 \sin^{n-3}\theta_1 d\theta_1 (s+t+u)^{n/2-1}. \tag{B14}$$

We have chosen the parameterization

$$k_1 = E_3(1, ..., \cos\theta_2 \ \sin\theta_1, \cos\theta_1) \tag{B15}$$

where the dots indicate $n-3$ components which we integrate over in a trivial way.

We introduce the change of variables $(\cos\theta_1, E_3) \to (v, w)$ with v and w defined as in (2.3). In the c.m system of the two incoming (massless) partons we have that $p_1 = Qn^+$ and $p_2 = Qn^-$ with $Q = \sqrt{s/2}$

$$n^{\pm} = \frac{1}{\sqrt{2}}(1, \mathbf{0}_\perp, \pm 1). \tag{B16}$$

From $t = (k_1 - p_1)^2 = -\sqrt{s}E_3(1-\cos\theta_1)$, $u = (k_1 - p_2)^2 = -\sqrt{s}E_3(1+\cos\theta_1)$ and using (2.3) we get

$$\cos\theta_1 = \frac{vw - 1 + v}{vw + 1 - v}$$
$$E_3 = \frac{\sqrt{s}}{2}(vw + 1 - v)$$
$$s + t + u = sv(1-w)$$
$$(1 - \cos^2\theta_1) = \frac{4(1-v)vw}{(vw+1-v)^2} \tag{B17}$$

and the jacobian of the transformation to be $\partial(\cos\theta_1, E_3)/\partial(v,w) = \sqrt{s}v/(1-v+vw)$. Therefore we obtain

$$PS_3 = \frac{\pi^{n-5/2}}{2^{n+1}\Gamma[n/2-1/2]\Gamma[n/2-2]} s^{n-2} \int dv dw (1-v)^{n/2-2}(1-w)^{n/2-1} v^{n-2} w^{n/2-2}$$
$$\times \int_0^\pi d\theta_1 \int_0^\pi d\theta_2 \sin^{n-1}\theta_1 \sin^{n-2}\theta_2. \tag{B18}$$

In order to compare this result with [20] we need an additional normalization factor $1/(2\pi)^{5-4\epsilon}$, due to the different definition of PS_3 we have adopted (now $n = 4-2\epsilon$) and we get

$$\begin{aligned} Ps_3 &\equiv \frac{1}{2\pi^{5-4\epsilon}} PS_3 \\ &= \frac{s^{2-2\epsilon}\pi^{1-2\epsilon}}{2^4(2\pi)^{5-4\epsilon}} \left(\frac{-\epsilon}{(1-\epsilon)}\right) 2^{3-2\epsilon} \int dvdw(1-v)^{-\epsilon}(1-w)^{1-\epsilon}v^{2-2\epsilon}w^{-\epsilon} \\ &\int_0^\pi d\theta_2 \sin^{2-2\epsilon}\theta_2 \int_0^\pi d\theta_1 \sin^{3-2\epsilon}\theta_1. \end{aligned} \tag{B19}$$

In order to integrate over the matrix elements, we need to evaluate the various scalar products which appear in such matrix elements, in the c.m. frame of the pair $(1,2)$. For this purpose we define the functions

$$\begin{aligned} P[x,y,z] &= (\frac{x^2+y^2+z^2-2xy-2yz-2xz}{4x})^{1/2} \\ E[x,y,z] &= \frac{x+y-z}{2\sqrt{x}}. \end{aligned} \tag{B20}$$

It is easy to show that

$$\begin{aligned} |p_1| &= P[s_{23}, p_1^2, u_1] \\ |p_2| &= P[s_{23}, p_2^2, t_1] \\ |k_3| &= |k_2| = P[s_{23}, p_1^2, p_2^2] \\ |k_1| &= \sqrt{\frac{s}{s_{23}}} P[s, k_1^3, s_{23}] \\ p_1^0 &= E[s_{23}, p_1^2, u_1] \\ p_2^0 &= E[s_{23}, p_2^2, t_1] \end{aligned} \tag{B21}$$

When all the external lines of the $2 \to 3$ process are massless, then we specialize (B21) as follows

$$\begin{aligned} p_1^0 &= E[s_{23}, 0, u_3] = \frac{s_{23}-u_1}{2\sqrt{s_{23}}} \\ p_2^0 &= E[s_{23}, 0, t_3] = \frac{s_{23}-t_3}{2\sqrt{s_{23}}}. \end{aligned} \tag{B22}$$

Now, using $t_3 = s(v-1)$ and $u_3 = -svw$ we get

$$p_1^0 = \frac{sv}{2\sqrt{s_{23}}}$$
$$p_2^0 = \frac{s(1-vw)}{2\sqrt{s_{23}}} \tag{B23}$$

In the massless case, the energies of the external final state particles are given by

$$k_1^0 = \sqrt{\frac{s}{s_{23}}} P[s, 0, s_{23}]$$
$$= \frac{1}{\sqrt{s_{23}}} \frac{(s - s_{23})}{2}$$
$$= \frac{1}{2\sqrt{s_{23}}} s(1 - v + w)$$
$$k_3^0 = k_2^0 = \frac{\sqrt{s_{23}}}{2}. \tag{B24}$$

In the derivation of (B24) we have used the relation $s + t_1 + u_1 = s_{23}$ together with (2.3). There are four different parametrizations of the integration momenta which we will be using. In the first one, which is suitable for unpolarized scattering [10], one defines (in the c.m. frame of the pair $(1,2)$)

- set 1

$$k_1 = \frac{1}{2\sqrt{s_{23}}} s(1 - v + w)(1, 0, ..., \sin\psi, \cos\psi)$$
$$k_3 = \frac{\sqrt{s_{23}}}{2}(1, ..., \cos\theta_2 \sin\theta_1, \cos\theta_1)$$
$$k_2 = \frac{\sqrt{s_{23}}}{2}(1, ..., -\cos\theta_2 \sin\theta_1, -\cos\theta_1)$$
$$p_1 = \frac{sv}{2\sqrt{s_{23}}}(1, 0, ..., 0, \sin\psi_2, \cos\psi_2)$$
$$p_2 = \frac{s(1-vw)}{2\sqrt{s_{23}}}(1, 0, ...0, \sin\psi_2, \cos\psi_2) \tag{B25}$$

where the dots denote the remaining $n-2$ polar components. Similarly, in the evaluation of the integrals over the hat-momenta we need the other parametrizations

- set 2

$$p_1 = p_1^0(1,0,...,0,0,1)$$
$$p_2 = p_2^0(1,0,...,-\sin\psi_2,0,\cos\psi_2)$$
$$k_1 = k_1^0(1,0,...,-\sin\psi_0,0,\cos\psi_0) \tag{B26}$$

- set 3

$$p_1 = p_1^0(1,0,...,\sin\psi_2,0,\cos\psi_2)$$
$$p_2 = p_2^0(1,0,...,0,0,1)$$
$$k_1 = k_1^0(1,0,...,\sin\psi_1,0,\cos\psi_1) \tag{B27}$$

- set 4

$$p_1 = p_1^0(1,0,...,\sin\psi_0,0,\cos\psi_0)$$
$$p_2 = p_2^0((1,0,...,-\sin\psi_1,0,\cos\psi_1)$$
$$k_1 = k_1^0(1,0,...,0,0,1) \tag{B28}$$

where $0,...$ refers to $n-5$ components identically zero. It is straightforward to obtain the relations

$$\sin\psi_0 = \frac{2\sqrt{w(1-v)(1-w)}}{1-v+vw}$$
$$\sin\psi_1 = \frac{2v\sqrt{w(1-v)(1-w)}}{(1-vw)(1-v+vw)}$$
$$\sin\psi_2 = \frac{2\sqrt{w(1-v)(1-w)}}{1-vw}. \tag{B29}$$

Which set of parametrizations we are going to use depends on the form of the hat-momenta which appear at the numerators of the matrix elements after the traces are performed.

Notice that

$$k_3 + k_2 = \sqrt{s_{23}}(1, \mathbf{0}). \tag{B30}$$

In the c.m. of the pair $(1,2)$ p_1, p_2 and k_1 lie on a plane, with the spatial components satisfying the condition $\mathbf{p_1} + \mathbf{p_2} + \mathbf{k_1} = 0$. Using (B25) and the expressions of t_1, u_1 and $s_{23} = sv(1-w)$ in terms of v and w, we can easily obtain the relations

$$\begin{aligned}
\sin\psi_2 &= \sqrt{\frac{1-w}{1-vw}} \\
\sin\psi_1 &= -\sin\psi\left(\frac{1-v-vw}{1-v+vw}\right). \\
\cos\psi &= \sqrt{\frac{w(1-v)}{1-vw}}
\end{aligned} \tag{B31}$$

Following Ref. [10] we introduce the variable

$$z = -\frac{k_3^\perp \cdot k_2^\perp}{(k_3^\perp)^2}, \tag{B32}$$

where the perpendicular components are measured in the c.m. system of the two incoming partons p_1 and p_2. We can covariantize (B32) in a trivial manner by using light cone identities

$$\begin{aligned}
k_3^2 &= 2k_3^+k_3^- - (k_3^\perp)^2 = 0 \\
(k_3^\perp)^2 &= 2k_3^+k_3^- = 2\frac{k_3\cdot p_1 k_3\cdot p_2}{p_1\cdot p_2}
\end{aligned} \tag{B33}$$

Similarly, expanding $k_3 \cdot k_2$ in its light cone components and covariantazing we get

$$k_3^\perp \cdot k_2^\perp = -k_3\cdot k_2 + \frac{k_3\cdot p_2 k_2\cdot p_1 + k_3\cdot p_1 k_2\cdot p_2}{p_1\cdot p_2} \tag{B34}$$

and

$$\begin{aligned}
z &= \frac{sk_3\cdot k_2 + uk_2\cdot p_1 + tk_2\cdot p_2}{tu} \\
&\equiv m\cdot k_2,
\end{aligned} \tag{B35}$$

where the four-vector m is defined by

$$m \equiv \frac{sk_3 + tp_2 + up_1}{tu}. \tag{B36}$$

(B35) is the covariant expression of z. At this point, however, it is necessary to evaluate m in the c.m. system of the pair $(1,2)$.

Using (B25) in Eq. (B36) it is a simple exercise to show that m has only longitudinal components given by

$$\begin{aligned} m &= (\frac{s}{tu})^{1/2}(\sqrt{\frac{w(1-v)}{1-w}}, 0, ..., 0, \sqrt{\frac{1-vw}{1-w}}) \\ &= (\frac{s}{tu})^{1/2}(m'_0, 0, ..., 0, m'_n). \end{aligned} \tag{B37}$$

Notice that $\cos\psi = m'_0/m'_n \equiv \tanh\chi$.

In order to isolate a pair $(1,2)$ of a given z, we introduce the identity

$$1 = \int dz\delta(z - m.k_2) \tag{B38}$$

in the expression of the phase space Ps_3 which becomes

$$\begin{aligned} Ps_3 = &\frac{s^{2-2\epsilon}\pi^{1-2\epsilon}}{2^4(2\pi)^{5-4\epsilon}2^8\Gamma[1-2\epsilon]}\left(\frac{-\epsilon}{(1-\epsilon)}\right)\int dvdw(1-v)^{-\epsilon}(1-w)^{1-\epsilon}v^{2-2\epsilon}w^{-\epsilon} \\ &\times\int_0^\pi d\theta_2 dz\delta(z - m\cdot k_2)\sin^{2-2\epsilon}\theta_2\int_0^\pi d\theta_1 \sin^{3-2\epsilon}\theta_1. \end{aligned} \tag{B39}$$

The integration over θ_1 can now be performed and the remaining δ-function eliminated. One gets

$$\begin{aligned} &\int_0^\pi d\theta_1 \sin^{3-2\epsilon}\theta_1\delta(z - m\cdot k_2) \\ &= \int_0^\pi d\theta_1 \sin^{3-2\epsilon}\theta_1\delta(z - 1/2 + 1/2\cos\theta_1 \coth\chi) \\ &= 2\ \tanh\chi g(v,w,z)^{1-\epsilon} \end{aligned} \tag{B40}$$

where

$$g(v,w,z) = \frac{1-w+4w(1-v)z(1-z)}{1-vw} \tag{B41}$$

The final phase space therefore can be cast in the form

$$\begin{aligned} Ps_3 = &\frac{\pi^{1-2\epsilon}s^{2-2\epsilon}}{2^4(2\pi)^{5-4\epsilon}}\left(\frac{-\epsilon}{(1-\epsilon)}\right)2\ \tanh\chi\ g(v,w,z)^{1-\epsilon}\int dv\,dw\,v^{2-2\epsilon}w^{-\epsilon}(1-w)^{1-\epsilon}(1-v)^{-\epsilon} \\ &\times\int_0^\pi d\theta_2 \sin^{2-2\epsilon}\theta_2 \end{aligned} \tag{B42}$$

APPENDIX C: EVALUATION OF THE PHASE SPACE INTEGRALS

From the definition of the hypergeometric function

$$F[a,b,c,z] = \frac{2^{1-c}\Gamma[c]}{\Gamma[b]\Gamma[c-b]}\int_0^\pi \frac{\sin^{2b-1}\theta(1+\cos\theta)^{c-2b}d\theta}{(1-z/2+z/2\cos\theta)^a} \tag{C1}$$

we easily get

$$I[a,2b-1] \equiv \int_0^\pi \frac{\sin^{2b-1}\theta d\,\theta}{(\alpha+\beta\cos\theta)^a} = \frac{\Gamma^2[b]}{\alpha^a 2^{1-2b}\Gamma[2b]}F[a/2,a/2+1/2,b+1/2,\beta^2/\alpha^2] \tag{C2}$$

We now use the relation

$$F[\alpha,\beta,\gamma,z] = (1-z)^{\gamma-\alpha-\beta}F[\gamma-\alpha,\gamma-\beta,\gamma,z] \tag{C3}$$

to get

$$I[2,2-2\epsilon] = \frac{\pi 2^{2\epsilon-2}}{\alpha^{1-2\epsilon}}\frac{\Gamma[3-2\epsilon]}{\Gamma^2[2-\epsilon]\,(\alpha^2-\beta^2)^{\epsilon+1/2}}F[1-\epsilon,1/2-\epsilon,2-\epsilon,\beta^2/\alpha^2], \tag{C4}$$

and

$$I[1,-2\epsilon] = \frac{\pi 2^{2\epsilon}}{\alpha^{-2\epsilon}}\frac{\Gamma[1-2\epsilon]}{\Gamma^2[1-\epsilon]\,(\alpha^2-\beta^2)^{\epsilon+1/2}}F[1/2-\epsilon,-\epsilon,1-\epsilon,\beta^2/\alpha^2]. \tag{C5}$$

At the end the result is expressed in terms of "plus" distributions using various identities whose derivation is briefly discussed in the next appendix.

For instance, let's denote by $Ps_3[t_3]$ the phase space contribution due to a factor $1/t_3$ in the matrix element. We get

$$Ps_3[t_3] = \frac{1}{t_{30}}K_{unp}\left(\frac{h^2}{g}\right)^\epsilon \frac{1}{|1-z|^{1+2\epsilon}}F[1/2-\epsilon,-\epsilon,1-\epsilon,\beta^2/\alpha^2]. \tag{C6}$$

where the factor K_{unp} is the same as calculated in the unpolarized case

$$K_{unp} = \frac{s^{1-2\epsilon}(4\pi)^{2\epsilon}2^{2\epsilon-8}}{\pi^3\Gamma^2[1-\epsilon]}(1-v)^{-\epsilon}(1-w)^{-\epsilon}v^{1-2\epsilon}w^{-\epsilon} \tag{C7}$$

Notice that at $z=1$, we have $\beta=\alpha$ and Taylor expanding the hypergeometric function around $z=1$ we get (with $r(z)\equiv\beta^2/\alpha^2$)

$$\begin{aligned} F[a,b,c,r(z)] &= F[a,b,c,1] + \frac{a\,b}{c}F[a+1,b+1,c+1,1]r'(1) \\ &= F[a,b,c,1] + (z-1)O(\epsilon). \end{aligned} \tag{C8}$$

Then we can set $F[a,b,c,r(z)] = F[a,b,c,1] + O(\epsilon)$ with $F[a,b,c,1] = 1/2^{2\epsilon} + O(\epsilon^2)$. We finally get (see appendix C)

$$Ps_3(1/t_3) = \frac{1}{t_{30}} K_{unp} \left(\frac{\theta(1-z)}{(1-z)_+} + \frac{\theta(z-1)}{(z-1)_+} + \delta(z-1)(-\frac{1}{\epsilon} - \log z_{max}) \right). \qquad \text{(C9)}$$

As an example of applications of of the methods discussed above in the polarized case, let's consider the contribution to the final phase space coming from matrix elements of the form $\hat{\vec{k}}^2/t_3^2$. We get

$$Ps_3\left(\frac{\hat{\vec{k}}^2}{t_3^2}\right) = \frac{1}{t_{30}^2} K_{pol} \left(\frac{-\epsilon}{2(1-\epsilon)}\right) \left(\frac{h^2}{g}\right)^{\epsilon} \frac{1}{|1-z|^{1+2\epsilon}} \eta(z) g(z) F[1-\epsilon, 1/2-\epsilon, 2-\epsilon, \beta^2/\alpha^2] \qquad \text{(C10)}$$

where

$$\eta(z) = \frac{1}{(1+\tanh^2 \chi(1-2z))} \qquad \text{(C11)}$$

and

$$K_{pol} = \frac{\pi^{2-2\epsilon} s^{2-2\epsilon} 2^{2\epsilon}}{2^6 (2\pi)^{5-4\epsilon}} \frac{\Gamma[3-2\epsilon]}{\Gamma[2-\epsilon]^2} v^{2-2\epsilon} w^{-\epsilon} (1-w)^{1-\epsilon} (1-v)^{-\epsilon} \qquad \text{(C12)}$$

For future purposes it is convenient to introduce the function $\sigma(z) \equiv \eta(z) g(z)$. We get

$$Ps_3\left(\frac{\hat{\vec{k}}^2}{t_3^2}\right) = \frac{1}{t_{30}^2} K_{pol} \left(\frac{-2}{1-\epsilon}\right) \delta(z-1) \qquad \text{(C13)}$$

$$Ps_3\left(\frac{\hat{\vec{k}}^2}{u_3^2}\right) = \frac{1}{u_{30}^2} K_{pol} \left(\frac{-2}{1-\epsilon}\right) \delta(z-1) \qquad \text{(C14)}$$

Notice that in the unpolarized case - as discussed in Ref. [10] - in some specific matrix elements, such as $Ps_3\left(1/(s_{13}u_3)\right)$, singularities in both variables v and w are encountered (for $w = 1$ and $z = 1$). The regularization in terms of plus-functions of the corresponding contributions and a detailed discussion of the derivation, which is similar to the polarized case can be found in Ref. [10].

APPENDIX D: IDENTITIES FOR "PLUS" DISTRIBUTION

As we have discussed before, we take z to be positive from the beginning.

In the expression of the final cross section, we are going to encounter singularities at $z = 1$ (and at $w = 1$) which have to be regulated in an appropriate way by the use of "plus" distribution. Identities for "plus" distribution can be easily derived by the integration by parts method, as we are going to illustrate briefly by an example. Assuming $z > 0$, we define two kinds of regulated "plus' distributions $\theta(1-z)/(1-z)_+$ and $\theta(z-1)/(z-1)_+$ by

$$\int_0^1 \frac{f[z]\theta(1-z)}{(1-z)_+}dz \equiv \int_0^1 dz \frac{f[z]-f[1]}{1-z}$$
$$\int_1^{z_{max}} \frac{f[z]\theta(z-1)}{(z-1)_+} \equiv \int_1^{z_{max}} \frac{f[z]-f[1]}{(1-z)}, \tag{D1}$$

Let's define the two functions

$$h(z) = \frac{1+\tanh^2\chi(1-2z)}{2\tanh\chi}$$
$$g(z) = \frac{1-w+4zw)(1-v)(1-z)}{1-vw} \tag{D2}$$

with $h(z_{max}) = -z_{min}$. Then we get the identities

$$\int_0^{z_{max}} dz f[z] \frac{\theta(z-1)}{(z-1)^{1+2\epsilon}} \left(\frac{h^2[z]}{g[z]}\right)^{\epsilon} = \int_0^{z_{max}} dz f[z] \left[\frac{\theta(z-1)}{(z-1)^{1+2\epsilon}} \left(\frac{h^2[z]}{g[z]}\right)^{\epsilon}\right]_+$$
$$+f[1]\left(-\frac{1}{2\epsilon} + \log(z_{max}-1) - \frac{1}{2}\log(\frac{h^2[1]}{g^2[1]})\right). \tag{D3}$$

We have integrated once by parts and the boundary (regular) terms have been set to zero before taking the limit $\epsilon \to 0$ and expanding in ϵ. The procedure has to be repeated once more if the boundary terms are still singular at the edge of the interval of integration. Now we use $z_{max} - 1 = -z_{min}$ together with the simple identity

$$\theta(z-1)\left[\left(\frac{h^2[z]}{g[z]}\right)^{\epsilon} \frac{1}{(z-1)^{1+2\epsilon}}\right]_+ = \theta[z-1]\frac{1}{(z-1)_+} + O[\epsilon] \tag{D4}$$

to finally obtain the relation

$$\theta(z-1)\left[\left(\frac{h^2[z]}{g[z]}\right)^{\epsilon} \frac{1}{(z-1)^{1+2\epsilon}}\right] = \theta[z-1]\frac{1}{(z-1)_+} + \delta(z-1)$$
$$\left(-\frac{1}{2\epsilon} + \log(-z_{min}) - \frac{1}{2}\log(\frac{h^2[1]}{g^2[1]})\right). \tag{D5}$$

In order to derive a similar identity in the case of $0 < z < 1$ we proceed in a similar way

$$\int_0^1 dz f[z] \frac{\theta(1-z)}{(z-1)^{1+2\epsilon}} \left(\frac{h^2[z]}{g[z]}\right)^{\epsilon} = \int_0^1 dz f[z] \left[\frac{\theta(z-1)}{(z-1)^{1+2\epsilon}} \left(\frac{h^2[z]}{g[z]}\right)^{\epsilon}\right]_+ + f[1] \left(-\frac{1}{2\epsilon} - \frac{1}{2}\log(\frac{h^2[1]}{g^2[1]})\right). \quad \text{(D6)}$$

Further manipulations similar to those presented above then give

$$\theta[1-z] \left[\left(\frac{h^2[z]}{g[z]}\right)^{\epsilon} \frac{1}{(z-1)^{1+2\epsilon}}\right] = \theta[1-z] \frac{1}{(z-1)_+} + \delta(1-z) \left(-\frac{1}{2\epsilon} - \frac{1}{2}\log(\frac{h^2[1]}{g[1]})\right). \quad \text{(D7)}$$

Combining (D5) and (D7), after some manipulations we get the identity

$$\frac{1}{|1-z|^{1+2\epsilon}} \left(\frac{h^2[z]}{g[z]}\right) = \frac{\theta(1-z)}{(1-z)_+} + \frac{\theta(z-1)}{(z-1)_+} + \delta(1-z)(-\frac{1}{\epsilon} - \log z_{max}). \quad \text{(D8)}$$

In a similar way we can derive the identity

$$\frac{1}{|z-1|^{1+2\epsilon}} \left(\frac{h^2(z)}{g(z)}\right)^{\epsilon} \eta(z) g(z) F[z] = \theta(1-z) \left(\frac{1}{1-z}\eta(z)g(z)\right)_+ + \theta(z-1) \left(\frac{1}{z-1}\eta(z)g(z)\right)_+ - \frac{1}{\epsilon}\delta(z-1)\,\eta(1)\,g(1)\,F[1] + \; O(1) \quad \text{(D9)}$$

Using $F[1] = 2(1 + O(\epsilon))$ where $F[z] \equiv F[1-\epsilon, 1/2-\epsilon, 2-\epsilon, r(z)]$ we get (C13) and (C14).

REFERENCES

[1] J. Ashman et al., EMC collaboration, Phys. Lett. **B206** (1988) 364, Nucl. Phys. **B328** (1989) 1.

[2] A. V. Efremov and O. V. Teryaev, Czech. Hadron Symposium (1988) 302; G. Altarelli and G. G Ross, Phys. Lett. **B212** (1988)391; R. D. Carlitz, J. C. Collins and A. H. Mueller, Phys. Lett. **B214** (1988) 229; G. Bodwin and J. Qiu, Phys. Rev. **D41** (1990) 391.

[3] SMC Collaboration, B Adeva et al. Phys. Let. **B302** (1993) 533, ibidem **B320** (1994)400; SMC Collaboration, D. Adams et al., Phys. Lett. **B329** (1994) 399; E143 Collaboration, K. Abe et al., SLAC-PUB-6508 (1994) preprint; E143 Collaboration, R. Arnold et al., presented at ICHEP94, Glasgow, August 1994.

[4] J. Ellis and R. Jaffe, Phys. Rev. **D9** (1974) 1444; Erratum **D10** (1974) 1669. (1989) 307.

[5] M. Anselmino, A. Efremov and E. Leader, Phys Rep. 261, NO.'s **1, 2**.

[6] E. B. Zijlstra and W. L. Van Neerven, Nucl. Phys. **B417** (1994) 61, Erratum **B245** (1994) 245. R. Mertig and W. L. Van Neerven NIKHEF-H/95-031. W. Vogelsang, Rutherford Preprint, RAL-TR-95-071.

[7] R. W. Robinett, ANL-HEP-CP-95-28, To appear in the proceedings of The International Symposium on Particle Theory and Phenomenology, Iowa State University, May 22-24, 1995.

[8] A. P. Contogouris, B. Kamal, Z. Merebashvili and F. V. Tkachov, Phys. Lett. **B304** 329 (1993); Phys. Rev. **D48** 4092 (1993). P. Ratcliffe, Nucl. Phys. **B223** 45, (1983).

[9] L. E. Gordon and W. Vogelsang Phys. Rev. **D48** (1993) 3136.

[10] P. Aurenche et al. Z. Phys. **C29**, (1985) 459. B. Bailey, J. Ohnemus and J. F. Owens

Phys. Rev. **D46**, 2018 (1992).

[11] M. A. Doncheski and R. W. Robinett, Phys. Rev. **D46**, 2011 (1992)

[12] C. Corianò and L. E. Gordon, to appear. While completing this work we found that new distributions for the polarized proton have been completed by Gluck et al., and Gehrmann and Stirling.

[13] J. F. Owens, Rev. Mod. Phys. **59**, 465 (1987).

[14] G. t'Hooft and M. Veltman, Nucl. Phys. B44, 189 (1972).

[15] P. Breitenlohner and D. Maison, Comm. Math. Phys. **52**, 11 (1977).

[16] G. Altarelli and G. Parisi, Nucl. Phys. **B126**, 298 (1977).

[17] m. Glück, E. Reya and A. Vogt, Phys. Rev. **D45**, 3986 (1992).

[18] H.-Y. Cheng and C. F. Wai, Phys. Rev. **D46**, 125 (1992).

[19] E. L. Berger, E. Braaten and R. D. Field, Nucl. Phys. **B239**, (1984) 52.

[20] R. K. Ellis, M. A. Furman, H. E. Haber and I. Hinchliffe, Nucl. Phys **B173** (1980) 397.

[21] G. Bonneau, Phys. Lett. **96B** 147 (1980).

Figure Captions

[1] (a) Lowest order Feynman diagrams for double prompt photon production. (b) Examples of single fragmentation contributions to double prompt photon production. (c) Example of box diagram contribution to double prompt photon production.

[2] (a) Examples of virtual corrections to the lowest order diagrams. (b) Examples of next-to-leading order three-body final-state diagrams for the $q\bar{q}$ initial state.

[3] Examples of contributions to the higher order qg initiated process.

[4] Unpolarized non-isolated cross section $d\sigma/dk_{T1}^{\gamma}dy_1dz$ as a function of z for $p+p \to \gamma+\gamma+X$ at $\sqrt{s} = 500$ GeV. We set $y_1 = 0$. Results are presented in the form of a histogram in bins of width $\Delta z = 0.2$. In (a), for $k_{T1}^{\gamma} = 5$ GeV, we show the net contribution from the lowest order process $q\bar{q} \to \gamma\gamma$ and from all the higher order processes and the full sum. In (b) we compare the polarized and unpolarized cross sections for the same parameters as in (a). The unpolarized has been multiplied by 0.1 for easier comparison.

[5] (a) The transverse momentum dependence of $d\sigma/dk_{T1}^{\gamma}dy_1dz$, the non-isolated cross section, for z integrated over the interval $0.2 < z < 2.0$. The upper solid line shows the full unpolarized cross section. The lower curves show the polarized cross section as given by the two different scenarios for the polarized parton distributions discussed in the text. (b) The longitudinal asymmetry, defined in the text, for the non-isolated cross section as predicted by parton distributions assuming scenarios a and b. The asymmetry for the lowest order Born cross section is included for comparison.

[6] (a) k_T dependence of the isolated cross section integrated over rapidity range $-3 \leq y \leq 3$ using isolation parameters given in the text. The unpolarized cross

section as well as the polarized cross section assuming scenarios a and b. (b) The longitudinal asymmetry for the cross section in (a) as predicted by scenario a and b. (c) The same asymmetry as in (b), but only for scenario a broken down into contributions from the $q\bar{q}$, qg and gg initiated processes.

[7] The renormalization/factorization scale μ dependence. For the sum of all contributing subprocesses, $d\sigma/dk_{T1}^{\gamma}$, for $-3 \leq y \leq 3$ is shown as a function of k_{T1}^{γ} for three values of $\mu = n((k_{T1}^{\gamma})^2 + (k_{T2}^{\gamma})^2)/2$: 0.5, 1.0, and 2.

[8] The same cross section as in fig.6a for the unpolarized case but with $\sqrt{S} = 14$ TeV.

FIGURES

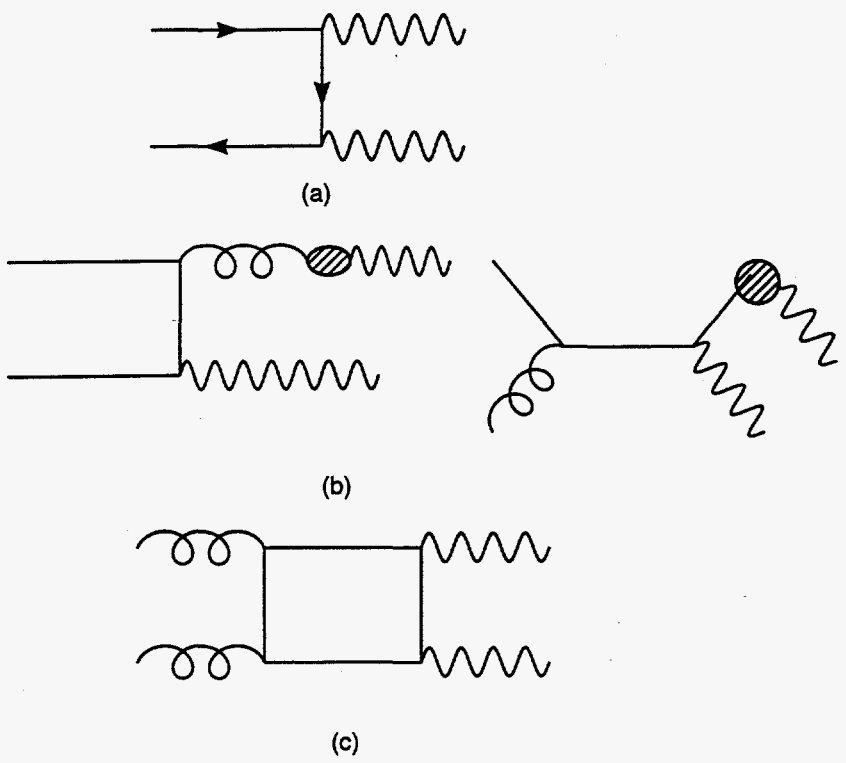

Fig. 1

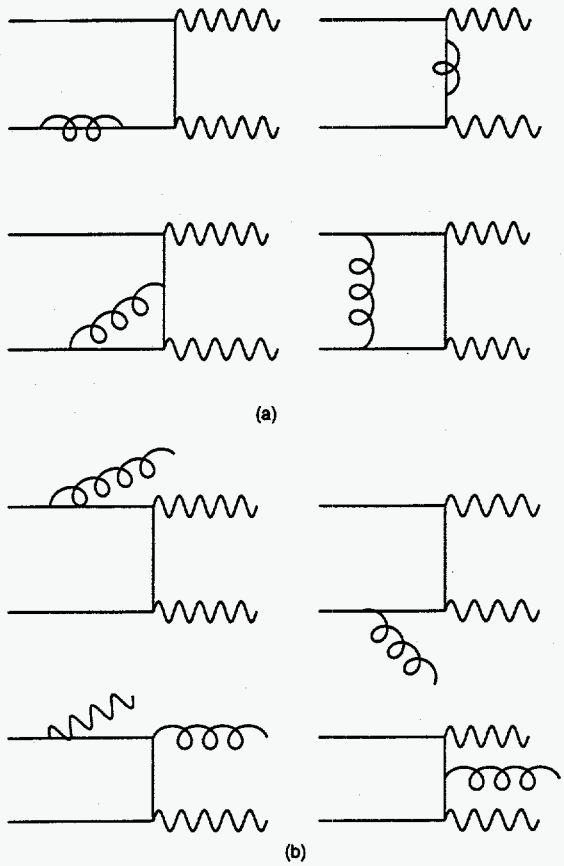

Fig. 2

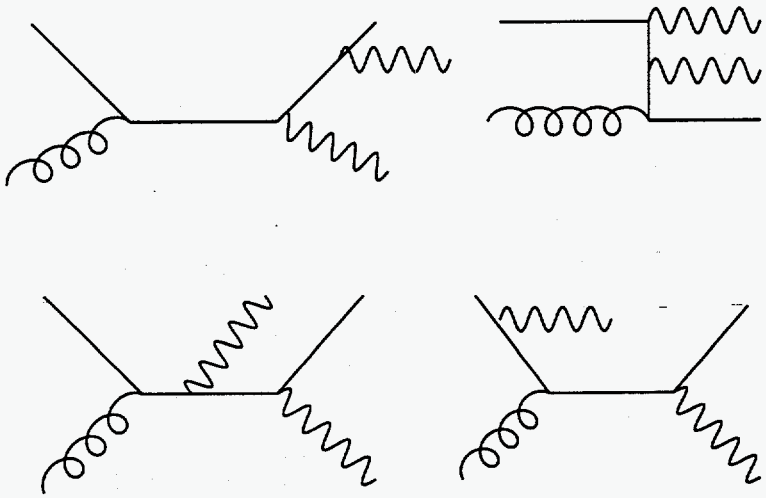

Fig. 3

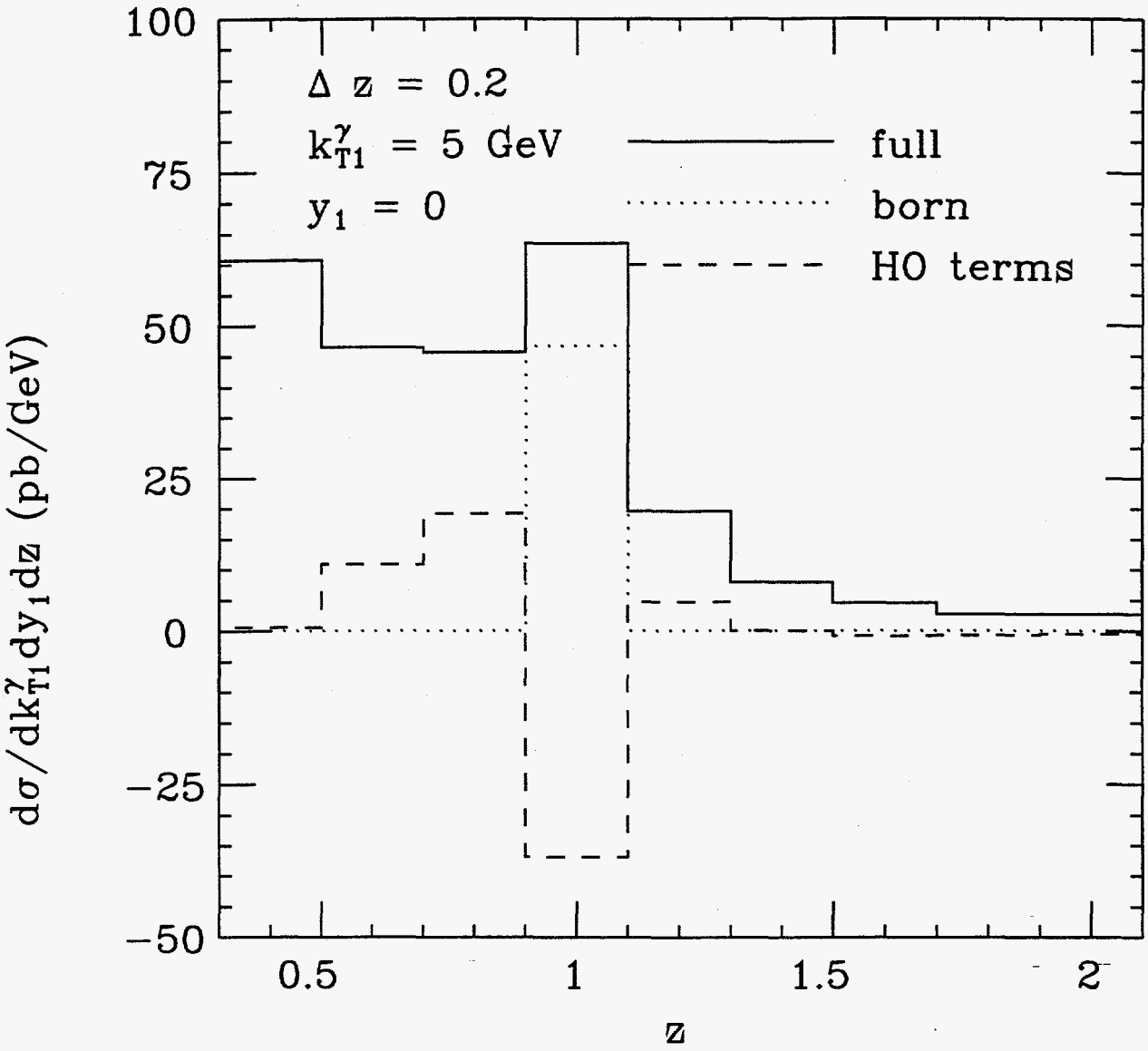
100
75
50
25
0
−25
−50
0.5
1
1.5
2
z
$d\sigma/dk_{T1}^{\gamma}dy_1dz$ (pb/GeV)
Δ z = 0.2
k_{T1}^{γ} = 5 GeV
y_1 = 0
full
born
HO terms

Fig. 4a

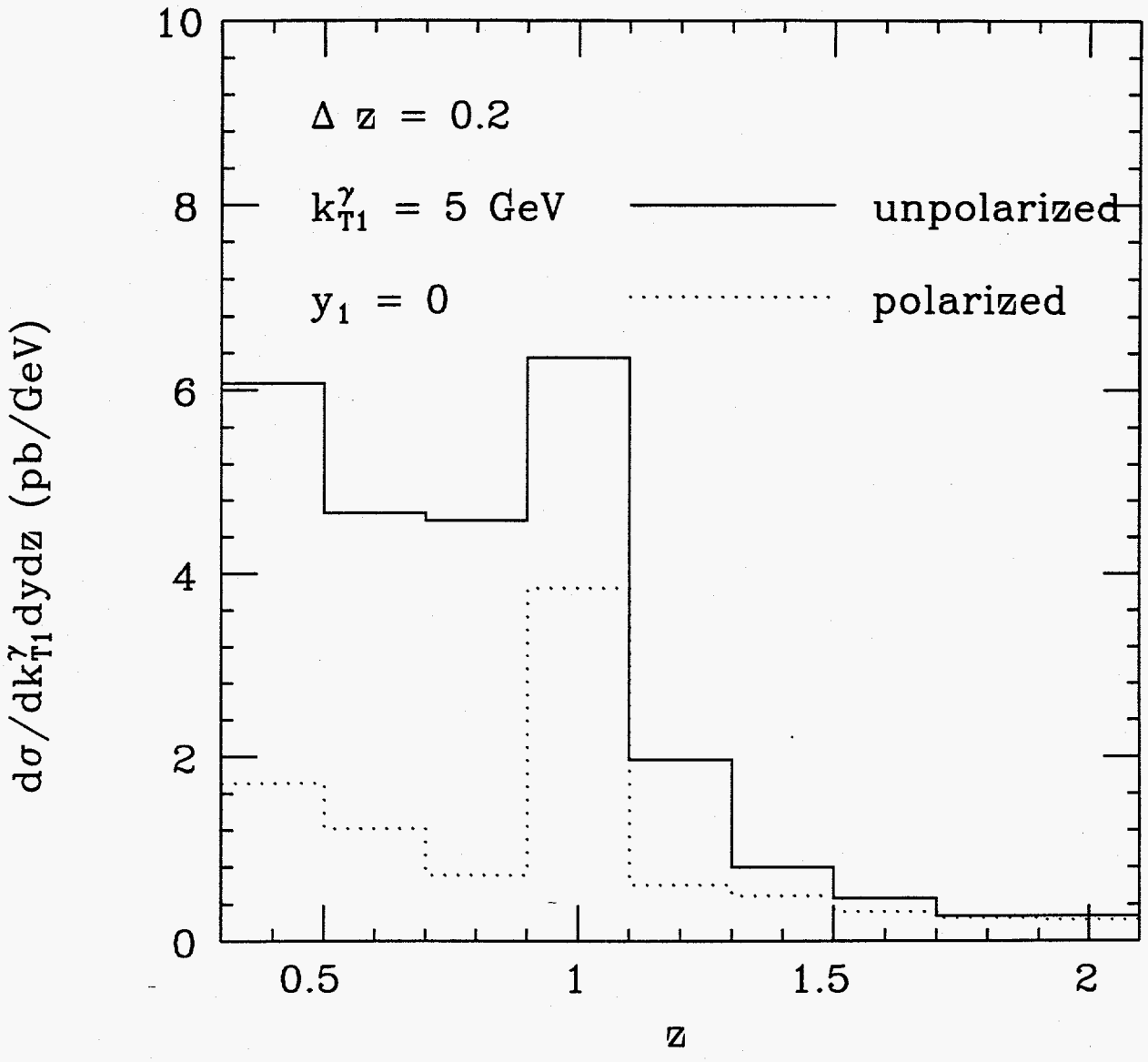
10
8
6
4
2
0
0.5
1
1.5
2
z
$d\sigma/dk_{T1}^{\gamma}dydz$ (pb/GeV)
Δ z = 0.2
k_{T1}^{γ} = 5 GeV
y_1 = 0
unpolarized
polarized

Fig. 4b

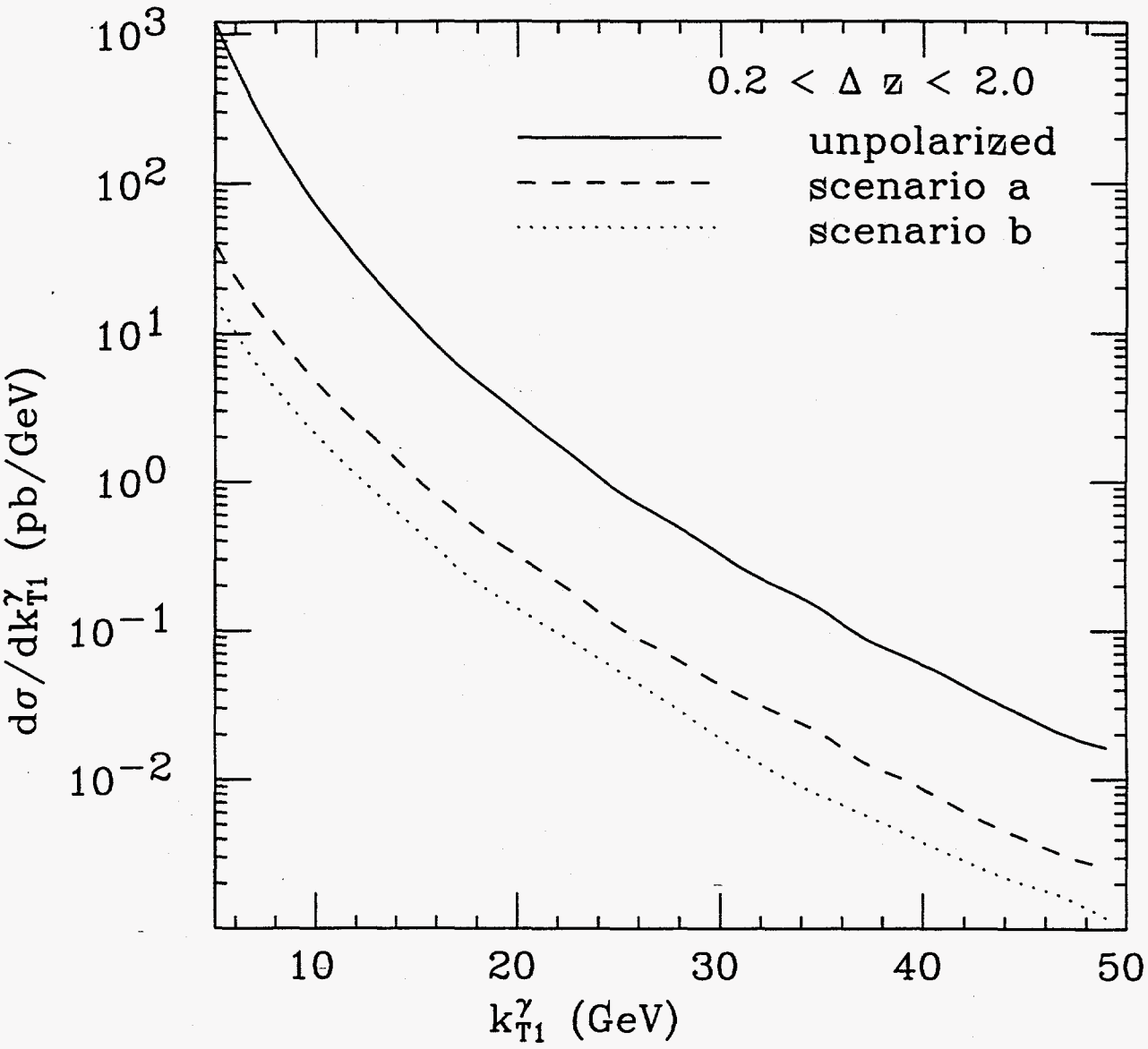
10^3
10^2
10^1
10^0
10^{-1}
10^{-2}
$d\sigma/dk_{T1}^{\gamma}$ (pb/GeV)
$0.2 < \Delta z < 2.0$
unpolarized
scenario a
scenario b
10
20
30
40
50
k_{T1}^{γ} (GeV)

Fig. 5a

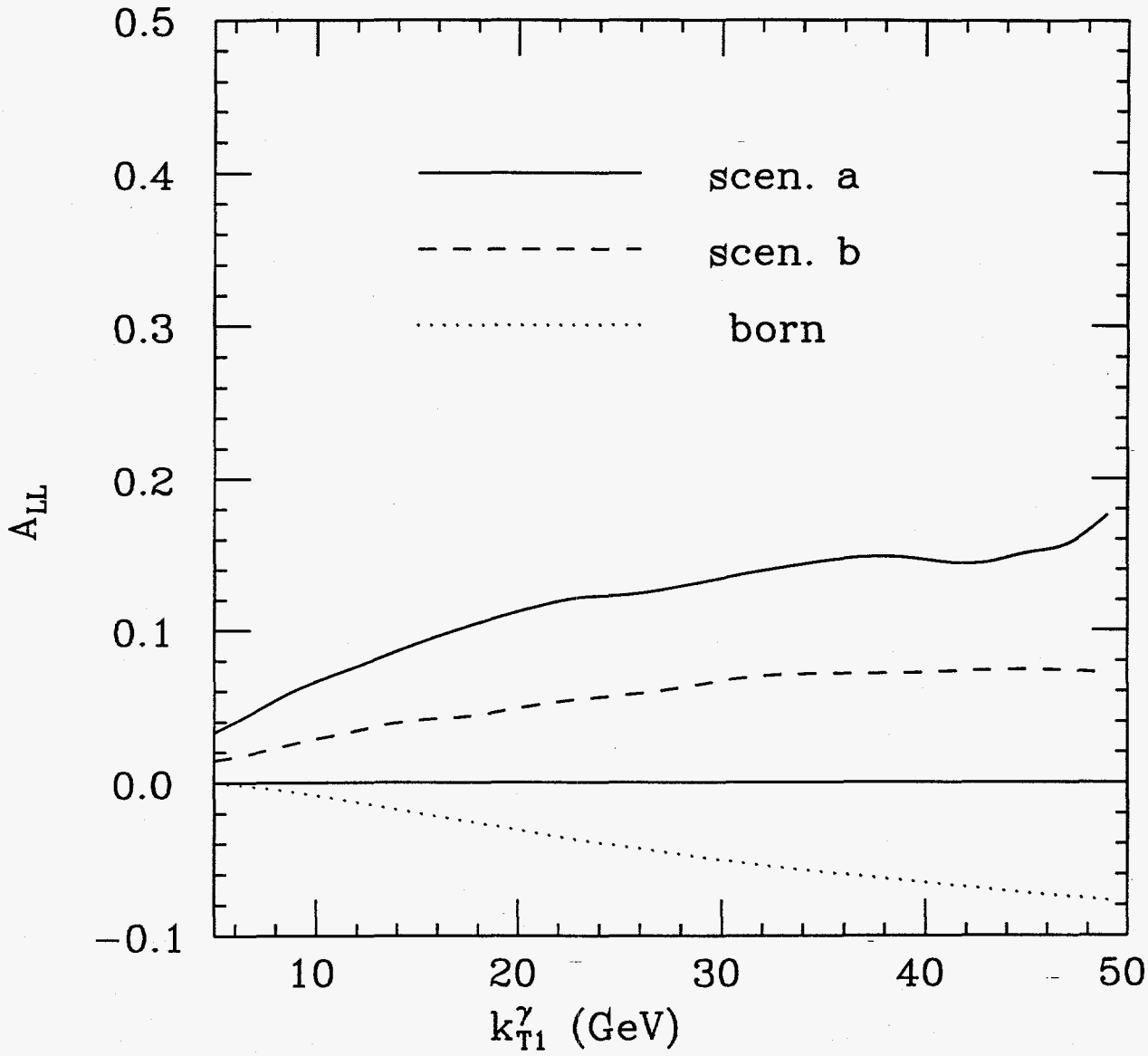
0.5
0.4
0.3
0.2
0.1
0.0
−0.1
A_{LL}
scen. a
scen. b
born
10
20
30
40
50
k_{T1}^{γ} (GeV)

Fig. 5b

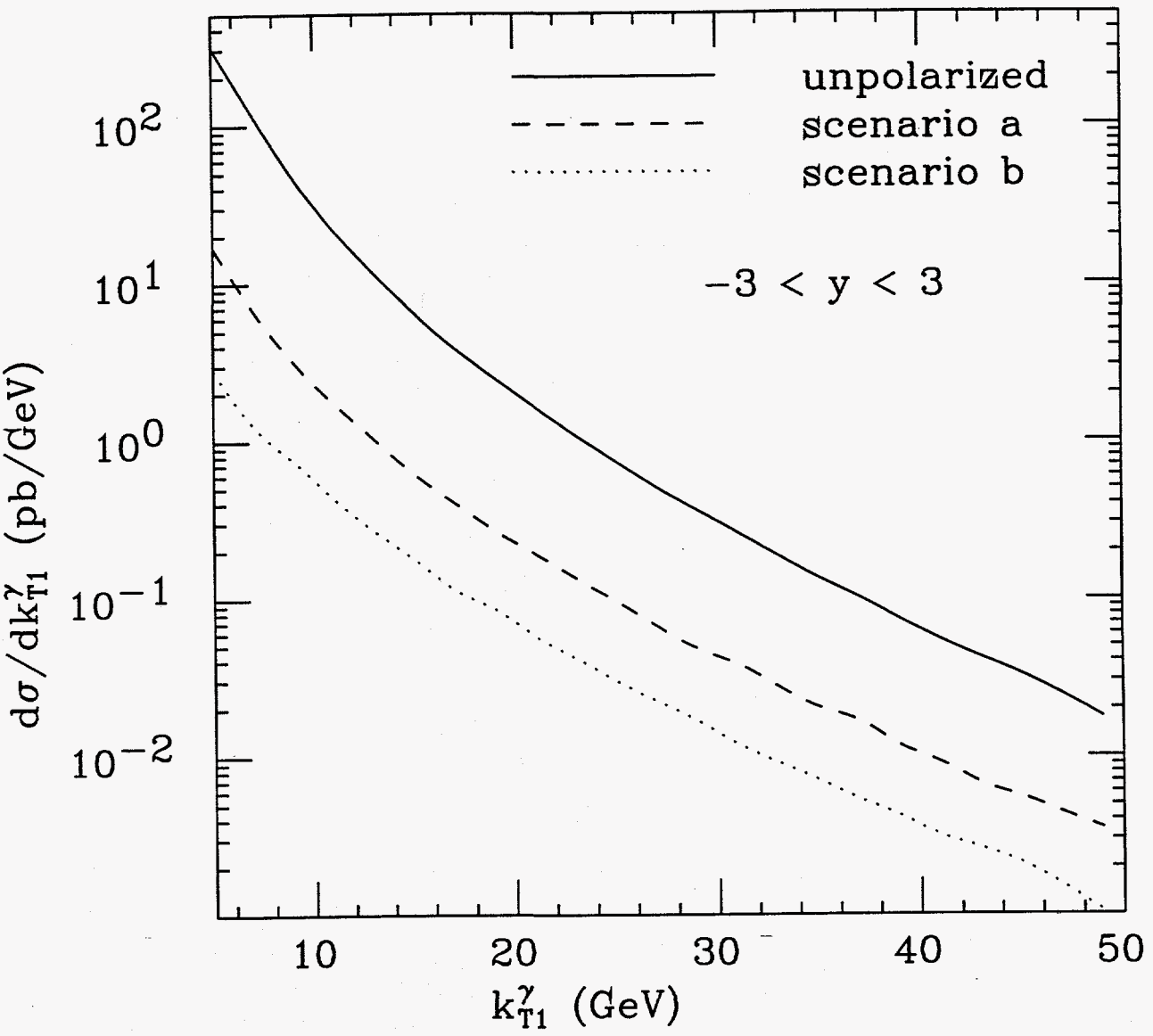
unpolarized
scenario a
scenario b
−3 < y < 3
10^2
10^1
10^0
10^{-1}
10^{-2}
$d\sigma/dk_{T1}^{\gamma}$ (pb/GeV)
10
20
30
40
50
k_{T1}^{γ} (GeV)

Fig. 6a

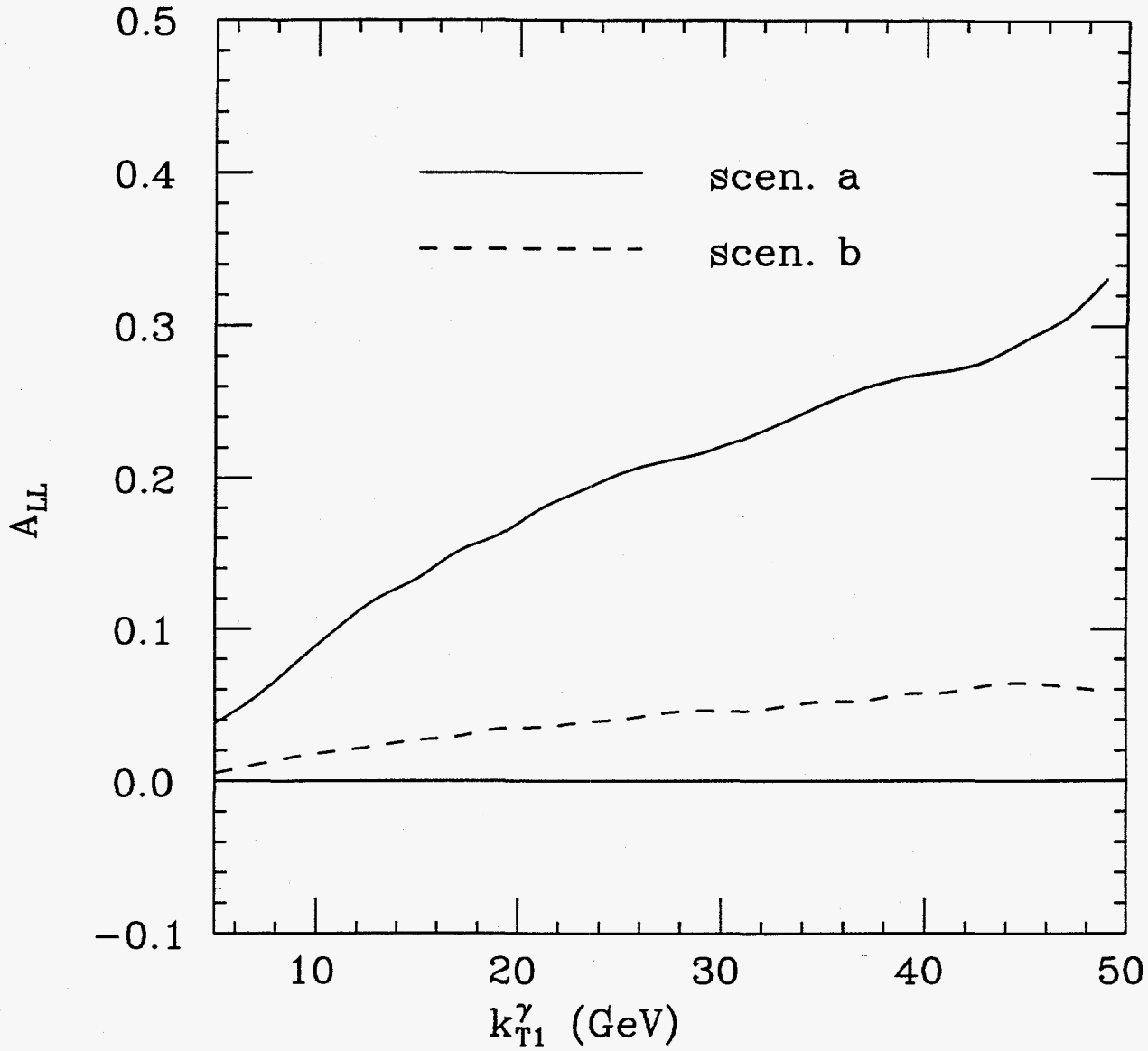

Fig. 6b

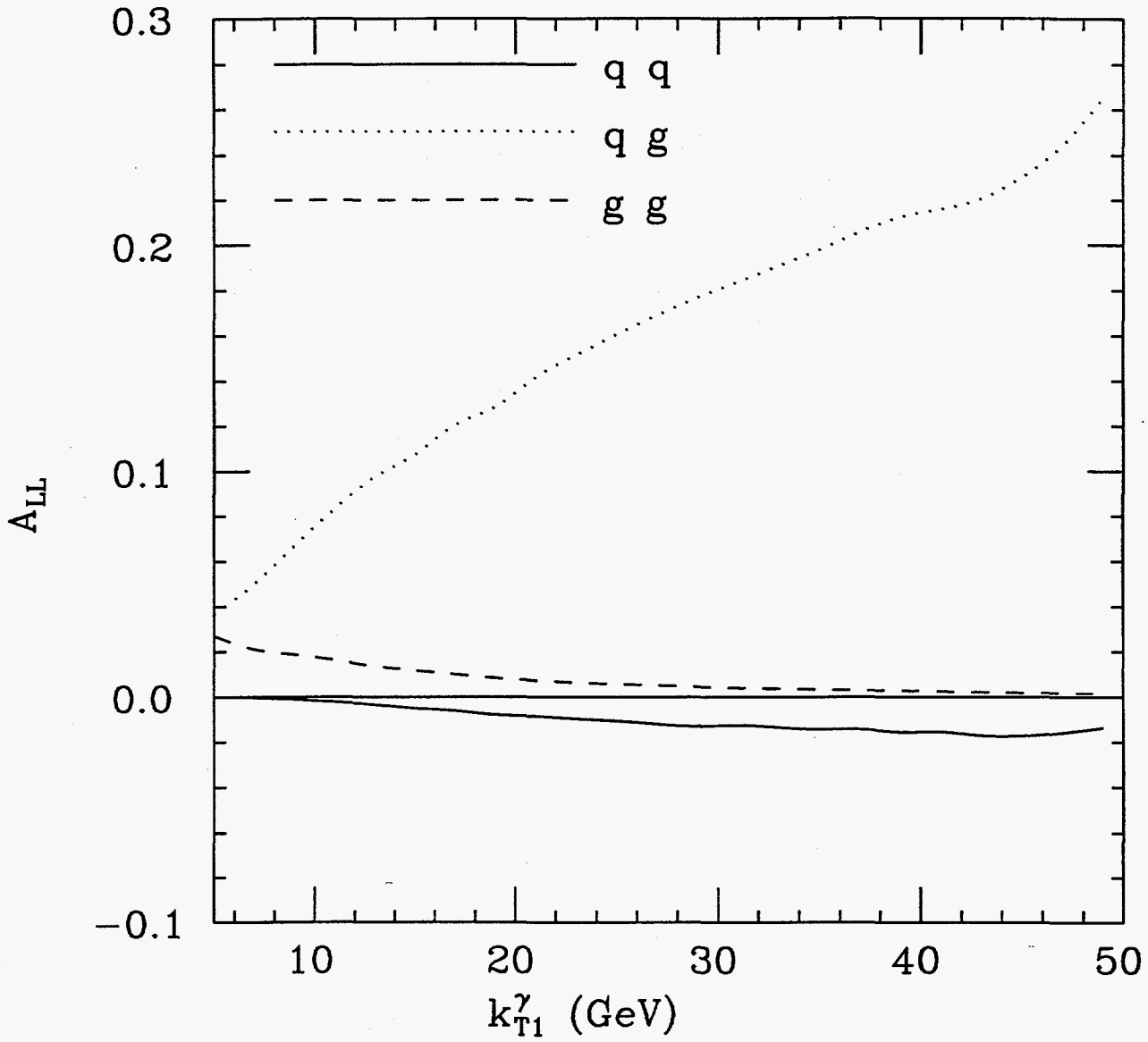

Fig. 6c

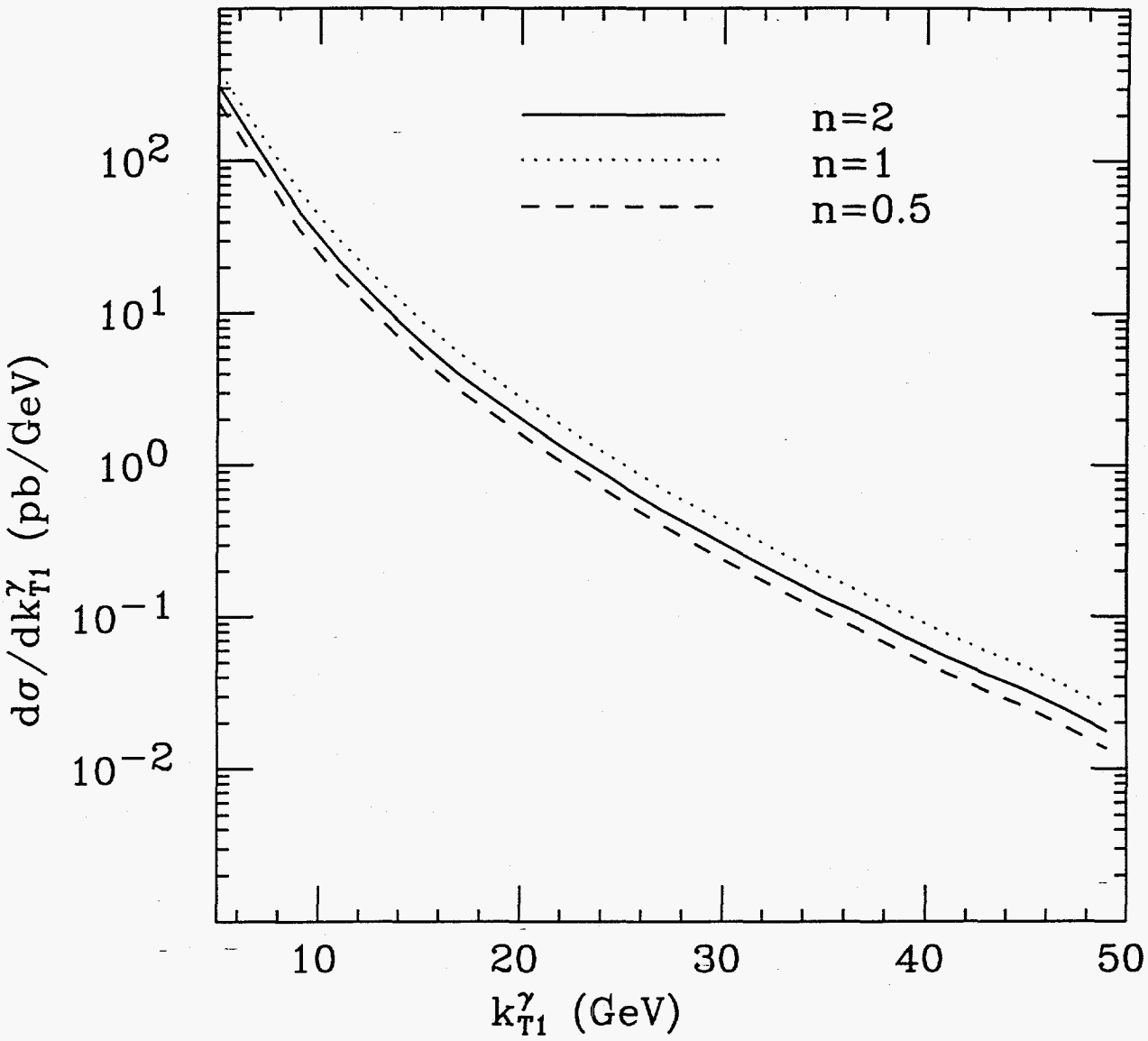
n=2
n=1
n=0.5
10^2
10^1
10^0
10^{-1}
10^{-2}
$d\sigma/dk_{T1}^{\gamma}$ (pb/GeV)
10
20
30
40
50
k_{T1}^{γ} (GeV)

Fig. 7

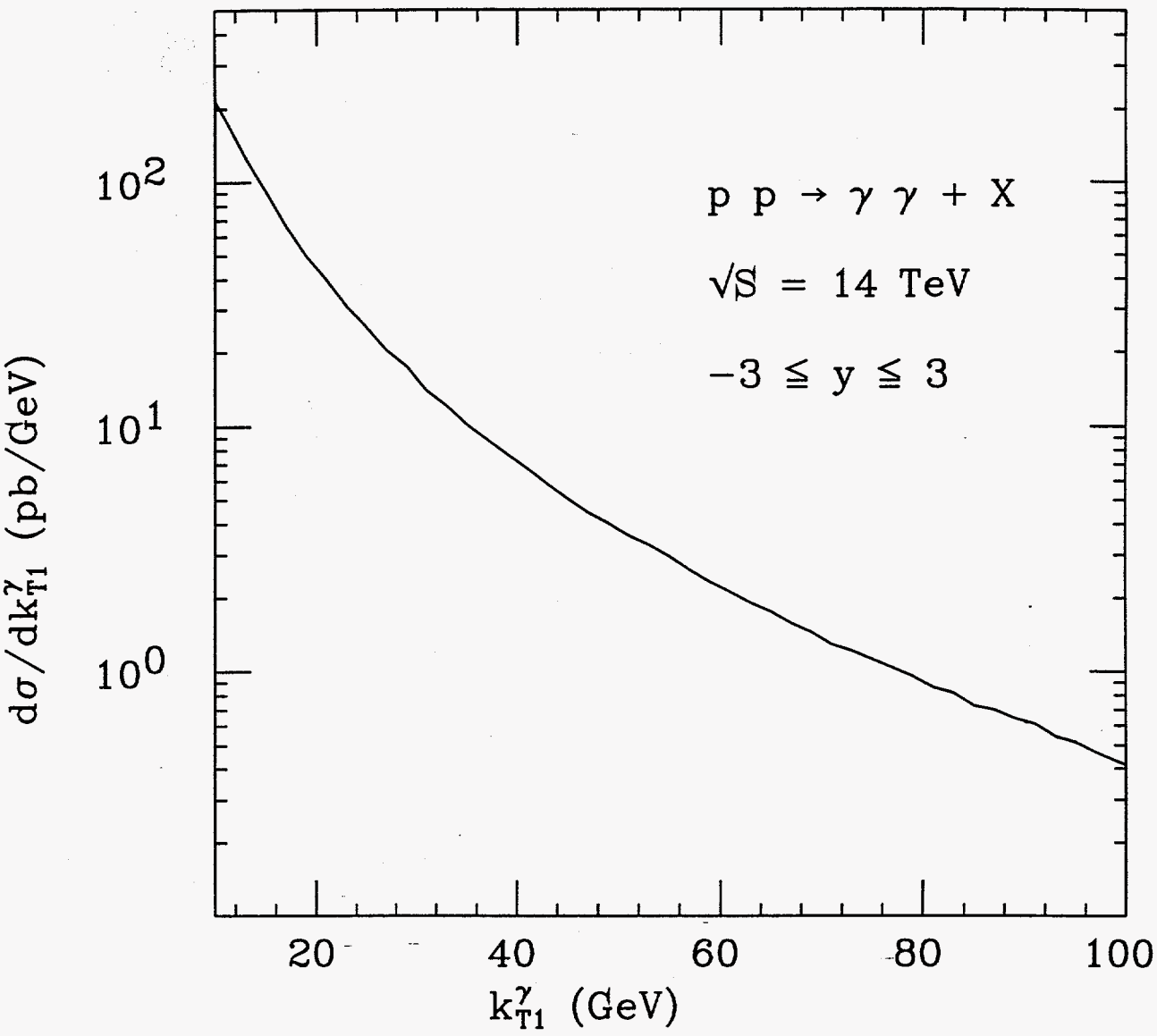
10^2
10^1
10^0
$d\sigma/dk_{T1}^{\gamma}$ (pb/GeV)
p p → γ γ + X
√S = 14 TeV
−3 ≦ y ≦ 3
20
40
60
80
100
k_{T1}^{γ} (GeV)

Fig. 8